UNLIMITED

TR 90046
ICAF 1776

ROYAL AEROSPACE ESTABLISHMENT

Technical Report TR 90046

September 1990

Fatigue Crack Closure - - A Review

by

R. M. J. Kemp

Procurement Executive, Ministry of Defence
Farnborough, Hampshire

UNLIMITED

0095421

CONDITIONS OF RELEASE

300216

.....

DRIC U

.....

DRIC Y

Reports quoted are not necessarily available to members of the public or to commercial organisations.

ROYAL AEROSPACE ESTABLISHMENT

Technical Report 90046
ICAF Document 1776

Received for printing 25 September 1990

FATIGUE CRACK CLOSURE - A REVIEW

by

R. M. J. Kemp

SUMMARY

The phenomenon of fatigue crack closure is now recognised as one of the most influential mechanisms operating during fatigue. This literature survey traces the development of research into fatigue crack closure and has been divided to present the two major approaches. The first part covers early work carried out between 1970 to 1980 which, broadly speaking, adopted a 'continuum' approach. The second part covers the period 1980 to 1988 when a mechanistic approach was widely adopted.

The survey has highlighted, firstly, the critical nature of experimental technique in the achievement of a meaningful measurement of crack closure load and secondly, that a diversity of mechanisms may operate to produce closure.

Particular attention has been given to crack closure in aluminium alloys and also to work relating crack closure to the corrosion fatigue situation.

Departmental Reference: Materials/Structures 294

LIST OF CONTENTS

		Page
1	INTRODUCTION	3
2	THE CONTINUUM APPROACH TO CRACK CLOSURE	4
	2.1 The discovery of crack closure	4
	2.2 The controversy over crack closure	5
	2.3 The importance of experimental technique	8
	2.4 Summary	17
3	THE MECHANISTIC APPROACH TO CRACK CLOSURE	21
	3.1 Plasticity-induced crack closure	21
	3.2 Roughness-induced crack closure	25
	3.3 Oxide-induced crack closure	28
	3.4 Crack tip shielding	33
4	MODELLING CRACK CLOSURE	34
5	THE EFFECT OF AN AQUEOUS LIQUID ENVIRONMENT ON CRACK CLOSURE	40
6	CONCLUSIONS	45
Table 1		47
References		48
Illustrations		Figures 1-9
Report documentation page		inside back cover

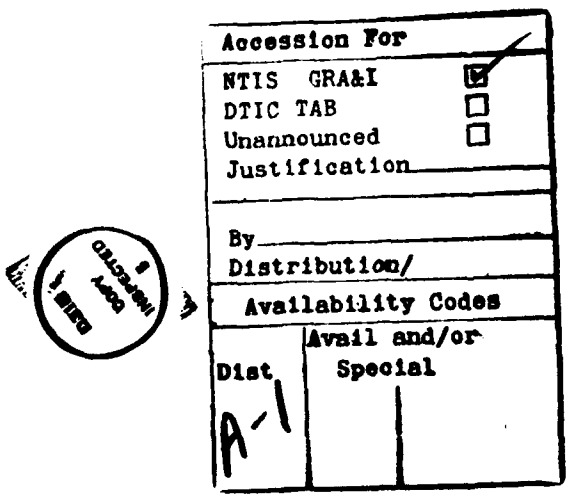

1 INTRODUCTION

The development and application of linear elastic fracture mechanics (LEFM) derived from Irwins[1] work in the 1950s has proved to be a powerful tool in the understanding of fatigue crack growth. For the LEFM approach, the material is considered to be an elastic continuum, and the stress condition at the tip of a crack is defined by a 'stress intensity factor', K, which is a function of applied stress, σ, and crack length, a. In 1963 Paris and Erdogan[2] used the LEFM approach to develop an effective representation for crack growth data by plotting crack growth rate (da/dN) against the stress intensity factor range, ΔK, *ie* $\Delta K = K_{max} - K_{min}$. A typical plot of crack growth rate is shown in Fig 1 with a central linear region for which they proposed the expression (generally known as the Paris law);

$$\frac{da}{dN} = C(\Delta K)^m$$

where C and m are constants.

This representation was effective in characterising the effect of maximum stress range on crack growth rate, but it was not able to include the effect of changing R-ratio (minimum/maximum stress). No suitable explanation for the 'R-ratio effect' was found until Elber[4] proposed the concept of 'crack closure'. He observed that the tip of a fatigue crack experienced a modified stress range compared to that calculated from the gross applied stress, due to a phenomenon of crack 'closure' at some load higher than the minimum of the loading cycle.

The importance of this finding on practical fatigue situations has gradually become recognised. For example, the effect of changing R-ratio, the effect of a short crack geometry, low ΔK crack growth (near-threshold) effects, and retardation due to an overload, have now been recognised as involving crack closure mechanisms which modify the stress intensity factor range experienced by the crack tip and hence the crack growth rate.

Historically speaking, there have been two approaches to crack closure which will form the basis for the major subdivision of the literature survey. Early work, between 1970 to 1980, assumed an elastic-plastic continuum in which the crack propagated and in which crack closure resulted from contact of residual plastic deformation in the wake of the crack tip. After 1980, a mechanistic

approach was adopted more widely and different closure mechanisms were identified. Many of these came to light as crack closure was investigated under different regimes of crack growth.

These two approaches will be reviewed with special emphasis on the long crack situation, followed by a review of the role of environment and of microstructure on crack closure effects, which will focus on aluminium alloys.

2 THE CONTINUUM APPROACH TO CRACK CLOSURE

2.1 The discovery of crack closure

In 1970, Elber[4] reported that a fatigue crack in a centre-cracked-tension (CCT) panel subjected to zero-to-tension loading was fully open for only a part of the loading cycle. Elber ascribed this to contact of residual plastic deformation in the wake of the crack tip and realised that these faces would be subjected to considerable compressive stresses.

Elber followed up his initial studies by looking at the effect of crack closure on fatigue crack growth rate[5]. He used 5mm thick CCT type specimens of aluminium alloy 2024-T3, and measured crack opening displacements at or near the crack tip using a surface-mounted displacement gauge. The load-displacement plot, measured 2 mm from the crack tip, was nonlinear as shown in Fig 2(a), and at the crack tip showed the behaviour as shown in Fig 2(b). The stress at which the crack opened fully was termed S_{op} , and for this material, Elber found S_{op} to be about 50% of S_{max} .

Elber interpreted the curves in Fig 2a and 2b as follows: between points A and B the relation was linear, and the stiffness was similar to the stiffness of the uncracked sheet. Between points C and D the relationship was also linear and the stiffness was the same as a sheet containing a sawcut of same length as the crack. He postulated that the curvature between B and C was due to closure effects. During unloading; the crack gradually closed between C and B and was fully closed between B and A. The differences shown by the clip gauge at the crack tip he explained by superimposed effects of plasticity. The negative curvature between D and E was due entirely to plastic deformation at the crack tip.

Elber postulated that crack closure was caused by the residual plastic tensile deformation left in the wake of the crack extension, shown schematically in Fig 3, which reduced crack opening and resulted in crack closure during unloading. Elber differentiated between the crack opening stress, S_{op} , and the

crack closure stress, S_{cl} , for the loading and unloading half cycles respectively and stated that S_{cl} would always be greater than S_{op} . Elber proposed that the crack tip stress intensity factor range, ΔK , would be modified by crack closure by a factor U , defined as $U = (S_{max} - S_{op})/\Delta S$.

The Paris law would then be expressed as:

$$\frac{da}{dN} = C(U\Delta K)^m$$

ie the lower the value of U the greater the crack closure effect.

2.2 The controversy over crack closure

Elber's proposal that crack closure occurred at discrete points on the fracture surfaces was supported by the work of Cheng and Brunner[6]. They used a polyester resin model of an SEN specimen to measure crack tip stresses by a photoelastic technique. After growing the fatigue crack under zero to tension loading, the specimen was unloaded and the residual birefringence pattern photographed. They found that upon unloading, localised residual compressive stresses were evident remote from the crack tip, indicating that the crack surfaces were in contact at discrete points. This confirmed Elber's findings that crack closure occurred at tensile loads.

A different experimental technique was used by Adams[7] for centre cracked 2024-T3 sheet specimens who used a high magnification photographic technique to measure crack opening displacement for various crack lengths. He confirmed Elber's results, and suggested that crack closure might account for the delay in crack extension due to an overload cycle, and also might reduce the ingress of a corrosive environment to the crack tip, hence reducing the corrosion fatigue effect. He measured a crack closure load of about 40% P_{max} .

Other workers, however, produced results that did not agree with Elber's results. Roberts and Schmidt[8] used a side surface mounted strain gauge technique to measure crack closure in 0.126 inch thick 2024-T3 and 0.25 inch thick 7075-T6 specimens. The strain gauge was bonded at each end straddling the crack tip of a compact tension specimen fatigued at $R = 0$. They recorded a crack closure load much lower than the 50% of P_{max} recorded by Elber, (*ie* around 25% of P_{max}), but were unable to explain the discrepancy, citing much lower ΔK levels used in their tests, and a compact tension specimen design compared to the centre-cracked tension specimen used by Elber.

Problems associated with the use of the electric potential method of crack closure measurement started to become apparent in the early work, and this led to much confusion over whether or not crack closure really existed.

Irving *et al*[9] used a potential method for Ti and Ti-6Al-4V and failed to observe crack closure in an air environment, but observed an effect if the pressure was below 10^{-3} torr. They proposed that the difference was due not to the test method but to the difference in crack tip plasticity in different environments.

Buck[10] described an ultrasonic method for detecting and measuring crack closure. The results were reported by Buck *et al*[11]. They used the ultrasonic surface wave technique on 12.5mm thick specimens of 2024-T851, 2024-T351, Al 2219, Ti-6Al-4V and 17-4 PH steel. Most of the results were obtained for 2024-T851 in a dry nitrogen environment for a part-through crack (*ie* elliptical) from a side notched specimen. They found that increasing σ_{max} at constant R led to an increase in crack closure. They reported that the results generally confirmed the presence of crack closure but that much more testing was required.

Bucci and Paris[12] cited a crack closure mechanism to explain their observation of the considerable effect of R-ratio on fatigue crack growth in Ti-8Al-1Mo-1V alloy in a dry argon atmosphere. Testing at $R = 0.05$ and $R = 0.125$ gave similar crack growth rates in approximately 6mm thick specimens, whereas testing at an R-ratio of 0.5 gave crack growth rates 2 or 3 orders of magnitude higher. They acknowledged that this effect could be explained by a crack closure argument, and noted that the slopes of the curves at all R-ratios were similar, and linear on a log-log plot.

Further support for the concept of crack closure resulted indirectly from the work of Hertzberg and Von Euw[13], who applied the crack closure concept to the estimation of crack growth from fracture surface striation spacing measurements. Using the formula due to Bates and Clark[14] for striation spacing, *ie*

$$\text{striation spacing} = 6\left(\frac{\Delta K}{E}\right)^2 ,$$

they incorporated the relationship due to Elber:

$$\frac{da}{dN} = C\,[0.5 + 0.4R(\Delta K)]^n .$$

This gave a modified expression for striation spacing in terms of ΔK_{eff} for the case of 2024-T3 as follows:

$$\text{striation spacing} \approx 24 \left(\frac{\Delta K_{eff}}{E}\right)^2 .$$

They found a better correlation of crack growth rate from striation measurement, when the effective stress intensity factor range was used.

Controversy soon arose over whether or not crack closure occurred under plane strain conditions. Ritchie and Knott[15] investigated the effects of mean stress on fatigue crack growth rate in medium and high strength steels. Examination of the fracture surfaces suggested that raising the mean stress in low fracture toughness steels could result in an increase in the static fracture component. They found evidence of cleavage, intergranular, and fibrous fracture modes in the lower toughness heat treatment variants. They found no evidence of crack closure due to a residual plastic deformation, and showed that in low fracture toughness materials, an R-ratio effect could be due to a change in fracture mechanism. They supported this conclusion by citing results obtained from work on the effect of mean stress on fatigue crack growth rate in aluminium alloys, since in alloys of toughness of the order of 40 MPa $\sqrt{m}$ there was a strong effect of mean stress[16,17] but in higher toughness alloys, no mean stress effect[23]. It is an important point to remember that during fatigue, cracking mechanisms may change which may affect crack growth rate.

Controversy also arose over whether or not the factor U was dependent upon K_{max}, the maximum applied stress intensity factor. Shih and Wei[19] for example studied crack closure in Ti-6Al-4V alloy using an electrical potential method and surface mounted strain gauges on centre-cracked tension specimens, 0.2 inch thick, and fatigue cracked at $R = 0.05$.

Electrical potential measurements were carried out in dehumidified argon to prevent surface oxidation effects. They found that crack closure was a function of R and K_{max}, and that no crack closure was observed for $R > 0.3$. U was unaffected by K_{max} at low load levels, was dependent on K_{max} at intermediate levels and only mildly dependent at high K levels. For constant R, they found that K_{op} increased with increasing K_{max}, but in such a way that U decreased. Shih and Wei proposed that the differences with Elber were due to the different materials studied, and because Elber's data were obtained at high

stress, *ie* above net section yielding. They found reasonable agreement between the two experimental techniques.

Using the same material but a different crack closure measurement technique, Katcher and Kaplan[25] did not observe the dependence of U on K_{max}. They used a crack tip opening displacement (CTOD) gauge technique on Ti-6Al-4V and found crack closure only for $R < 0.35$. They found that U is independent of K_{max} for constant R, and U increased with R according to the relationship $U = 0.73 + 0.82R$ (in normal air).

One factor which might explain the discrepancies noted above was the difference in environment used by the two sets of researchers - dry argon by Shih and Wei, and normal air by Katcher and Kaplan. The use of dry argon by the former was to overcome problems observed by earlier workers in that oxidation of the fracture surfaces formed an electrically insulating layer which masked crack closure effects. This produced anomalous crack closure results.

2.3 The importance of experimental technique

The work of Lindley and Richards[21] assisted greatly in unravelling the controversy over whether or not crack closure occurred under plane strain conditions. They investigated the effects of specimen thickness on crack closure measurements, and were among the first workers to identify the dependency of crack closure results on experimental technique. They pointed out that markedly different values of crack closure load had been measured by different techniques and set out to show that measurements from the specimen surface (plane stress region) differed from the results of bulk measurements effects (plane strain region). They tested 0.8, 1.6, 7.7 and 19.5mm thick specimens of spheroidised 1% carbon steel using the bulk effect measurement techniques of dc and ac potential drop combined with a surface mounted COD gauge. In thick specimens for zero to tension loading, they detected crack closure only if a compressive load was applied, but for tension-tension fatigue loading, crack closure occurred at tensile loads less than P_{min}, but greater than zero. For thin specimens (0.8 and 1.6 mm thick), however, they observed that crack closure occurred at load values higher than P_{min}. The values of crack closure load were much lower when measured using a dc technique compared to values measured using a surface-mounted clip gauge. Sectioning of the specimens showed that it was the outside edges of the fracture faces - the shear lips - that were contacting at the crack closure load whereas the central plane strain region remained open. They concluded that for the plane strain situation, crack closure measurement techniques that

measured crack closure at the specimen faces were unrepresentative of the plane strain situation within a thick specimen. They further postulated from their results that crack closure did not occur at tensile loads under plane strain conditions.

Pitoniak *et al*[22] confirmed the observations of Lindley and Richards and provided additional information on the crack closure mechanism in thick section specimens by using a direct observation technique. They used a monochromatic light interferometry technique on compact tension specimens (B = 19 mm) of polymethyl methacrylate (PPMA or 'Perspex'). Fatigue cracks were grown under constant ΔK loading, and when the loading was removed, the interference fringe pattern indicated that crack closure occurred around the entire perimeter of the fatigue fracture surfaces - along the crack tip, along the surface edges and along the tip of the notch.

Upon applying a tensile load they observed that the crack faces separated first at the centre of the specimen at the notch tip, separation progressed along the notch tip towards the specimen edges, then along edges to the crack tip. It is noted that crack closure near the notch tip might be due to the high loads used to start the fatigue crack.

Further work on the effect of K_{max} on crack closure was reported by Bachmann and Munz[23], who used CT specimens (B = 12.7 mm) of Ti-6Al-4V CT specimens, and a COD gauge on the mouth or side of the specimen. They found that K_{op} was independent of K_{max}, and that U increased with increasing K_{max}. K_{op} was found to increase with increase in R; $K_{op} = 4.6$ MN $m^{-3/2}$ for $R = 0.05$; and $K_{op} = 5.6$ MN $m^{-3/2}$ for $R = 0.2$.

Assuming a linear relationship between K_{op} and R, they proposed the expressions

$$K_{op} = 6.67R + 4.27$$

$$U = \frac{1}{1 - R}\left[1 - \frac{6.67R}{K_{max}} - \frac{4.27}{K_{max}}\right].$$

In both air and vacuum, they observed that K_{op} was independent of the environment. They criticised the work of Irving *et al*[9] saying that the potential method was affected by air pressure.

The result that K_{op} was independent of K_{max} disagreed with the results of Shih and Wei[19] and Irving *et al*[9]. These workers used an electrical potential method in argon. In vacuum, Bachmann and Munz found that K_{op} measured by the potential method was higher than K_{op} measured with displacement gauge.

Irving *et al*[24] defended their earlier results in response to the comments of Bachmann and Munz and pointed out that the surface measurement technique of Bachmann and Munz[23] did not measure the situation in the centre of a thick specimen. They questioned whether the effective ΔK concept had any validity in the plane strain situation. They proposed that R-ratio effects were better understood in terms of environmental influences or by subcritical cracking as suggested by Ritchie and Knott[25].

Irving *et al*[26] carried out further work using a potential drop technique and crack mouth compliance method to measure crack closure on EN24 steel and several titanium alloys in vacuum. They found good agreement between the PD and CMOD compliance methods, and were the first to use an offset method with a clip gauge (*ie* a null deflection method; they subtracted a back-off voltage from the clip gauge signal so that the signal could be highly amplified).

For 5mm thick titanium centre-cracked tension specimens, they measured the variation of potential and plotted their data as percentage of crack area closed since the potential method measures the area of uncracked ligament, modified by crack closure effects. For an R-ratio of 0.35, the nominal crack closure initially increased with increasing crack length (a/W) to a peak of 10% at $(a/W) = 0.3$ then decreased to 2-3% at (a/W) of 0.5 to 0.6. Testing different titanium alloys under the same conditions showed the same trends but different percentages of nominal crack closure. Varying the R-ratio had a marked effect on the nominal percentage crack closure vs crack length curves. At $R = 0.7$, percentage nominal crack closure (PNC) was less than 1%, compared to 10% at $R = 0.07$ and $a/W = 0.25$. Increasing crack length at $R = 0.07$ led to a marked increase in PNC to over 40% at $a/W = 0.5$ to 0.6. The authors also examined the effect of air pressure on nominal crack closure. As air pressure decreased, the amount of crack closure decreased, gradually at first, and finally disappeared between 10^{-3} and 10^{-2} torr (0.133 and 1.33 MPa). In air, from the COD vs load measurements, crack closure was observed as the load dropped below minimum load, P_{min}, whereas in vacuum, crack closure was observed below mean load, P_{mean}. A considerable effect of environment was therefore observed, which the authors explained in terms of the environment affecting the extent of

plastic deformation at the crack tip. They also noted, however, that the amount of crack closure occurring above minimum load in vacuum was seen to be small in comparison with the degree of crack closure produced by reducing the load below the cyclic minimum (10% PNC at P_{min} in vacuum, 0% in air; 41% PNC at zero load in vacuum, 31% in air). The amount of crack closure (*ie* percentage of fracture faces contacting) was always higher in vacuum.

Another attempt to clarify the extent of crack closure by using surface and bulk measurement techniques simultaneously was carried out by Frandsen *et al*[37]. They used acoustic and strain gauge techniques simultaneously on part through crack (PTC) test pieces (elliptical surface crack) and compact tension (CT) test pieces of aluminium alloy 2219-T851. An acoustic surface wave technique was used on the PTC specimen and a longitudinal bulk wave technique on the CT specimen, using both the transmitted and the reflected acoustic beam. Two compliance gauges were used on the CT test piece; a conventional crack mouth opening displacement (CMOD) gauge and an Elber type gauge (side face mounted). Testing was carried out in air at R values of 0.08, 0.3 and 0.5. At low R values, the crack closure point measured by the acoustic bulk wave signals agreed well with that measured by the Elber gauge. As the R value was increased, however, they found that it became more difficult to determine the crack closure load P_0 using the Elber gauge. They observed crack closure at $R = 0.5$ using the acoustic technique but not using the Elber gauge. They found furthermore that both the sensitivity and the crack closure load varied with the relative location of the Elber gauge. At low R they found that agreement between acoustic technique and Elber gauge was best with the gauge 2.5 mm behind the crack tip.

At low levels of K_{max}, (7-11 MPa $\sqrt{m}$), the crack closure load was found to decrease with increasing K_{max}, and above 10 or 11 MPa $\sqrt{m}$ became constant. This result, when used to plot crack growth rate against ΔK_{eff} ($= K_{max}(1 - P_0/P_{max})$) showed that the growth rate no longer tended towards a threshold value.

Gomez *et al*[28] attempted to check the validity of Elber's results, and used wedge-opening load (WOL) specimens of 2024-T3, 4.3 mm thick. They measured crack closure by the method of Roberts and Schmidt[8] as described previously. They found that for R-ratios of 0.2, 0.45 and 0.7, a plot of ΔK_{eff} against ΔK gave reasonable agreement with Elber's results and concluded that the expression derived by Elber for ΔK_{eff} ; *ie*

$$\Delta K_{eff} = \Delta K(0.5 + 0.4R)$$

was a valid expression.

Shih and Wei[29], however, replotted the data of Gomez *et al*[28] in terms of U vs K_{max} . They refuted the claim that the results supported the validity of Elber's equation for U , and suggested that the data rather showed a systematic deviation indicating that U increased with increasing K_{max} for the three R-ratios studied. Hence they claimed that the latter results[28] contradicted rather than supported Elber's results and also those of their own earlier work[19].

Clarke and Cassatt[30] compared crack closure measurements made using a crack-tip compliance gauge and an electric potential technique on 7075-T651 centre-cracked panels of thicknesses 6.4, 12.7 and 25.4 mm. Tests were carried out in high purity argon and a partial vacuum to retard fracture surface oxidation. Comparable results from the potential and crack-tip gauge results were produced. Closure was observed to be a function of specimen thickness, R-ratio and K_{max} , but not crack length. U was observed to increase with increasing K_{max} for 6.35 and 25.4mm thick specimens, but decreased for the 12.7mm thick specimen. Closure measurements gave an average value of $U = 0.8$. A significant observation was that protuberances on the fracture surface were detected by the potential system but these appeared not to affect the compliance measurements. This observation provided a further explanation for differences between crack closure measured by different measurement techniques. It also added the complication that contact between fracture surfaces could occur that did not affect the crack-tip stresses. This was later to be described by other workers in terms of 'local' and 'global' crack closure phenomena.

The value of U that they measured differed from that observed by Elber, and Clarke and Cassatt explained this result by pointing out the effect of specimen geometry, material type and the lower range of stress intensity values used. The possible effect of environment was not mentioned.

Garrett and Knott[31] questioned the validity of crack closure data, since results had varied so much, and results from different measurement techniques - electrical potential compliance and acoustic - had differed widely. They analysed data obtained in earlier work[32] to investigate the effects of crack-tip plasticity on crack-growth rate. The work was carried out on 10mm thick SEN bend specimens of 2014 in naturally and peak-aged conditions to determine the effects on crack-growth rate of annealing out the cyclic hardened plastic zone at the crack tip after fatigue loading ($R = 0.33$, $\Delta K = 20$ MPa$\sqrt{m}$). For the peak-aged

(T6) condition, fatigue crack growth rate was identical before and after annealing. They concluded that growth rate was controlled by a strain hardening mechanism at the crack tip, and that crack closure had little if any effect under plane strain conditions.

Shaw and Le May[33] determined crack closure loads on single-edge notched (SEN) specimens of AISI 4140 steel. They used a surface displacement strain gauge technique and crack opening displacement gauge to measure crack closure, in addition to examining replicas taken from the side faces and fracture surfaces. They defined the crack opening load, P_{op} , as the load at which the crack tip was fully open or the point at which the crack tip was on the verge of closing. The crack closure load, P_{cl} , was defined as the load where the entire length of the crack no longer experienced any further crack closure with reduction of applied load - *ie* a measure not of the crack-tip crack closure, but of the natural crack closure of the entire crack. These points were the transitions between linear and nonlinear compliance and were found to be independent of the direction of loading.

Examination of fracture surface replicas showed that crack closure contact between the surfaces occurred only in the slant fracture regions, not in the centre of the specimens, in agreement with the results of Lindley and Richards[21]. They found that using a crack-tip opening displacement (CTOD) gauge, the value of crack opening load was dependent upon the distance from the crack tip, being higher at distances less than about 2.5 mm. By correcting for the effect of surface strains, calculated from finite element analysis, they explained the effect of measurement position in terms of a surface strain component close to the crack tip. Increasing crack length produced a slight decrease in crack-opening load ratio (P_{op}/P_{max}), although the authors considered it insignificant and concluded that U was independent of crack length.

Since the crack opening and crack closure loads were largely due to shear lips, Shaw and Le May[33] commented that changes in parameters that affected slant mode fatigue, such as environment, specimen thickness, loading conditions, material properties and possibly frequency, would significantly affect crack closure.

Bachmann and Munz[34] examined crack closure in 12.7mm thick compact tension specimens of Ti-6Al-4V using the electric potential, crack mouth (CMOD) and crack tip (CTOD) displacement gauges. In vacuum, a different value of opening load, P_{op} , was obtained using a CTOD gauge. In air, they observed a much smaller

total change of potential reading during one cycle than in vacuum. They explained this in terms of the insulating effect of the oxide layer formed. The opening load measured by the potential and CTOD extensometer techniques was similar. The effect on crack closure of changing the environment from vacuum (5×10^{-4} torr) to 760 torr and vice versa was investigated. The change in potential difference after these changes was not instantaneous but took up to 100 cycles to complete. The total change in potential difference was reduced on changing from vacuum to atmospheric pressure, and was increased on changing from high to low pressure. They explained this effect in terms of a mechanism of progressive oxide formation/destruction, with the load cycling process helping to increase the thickness of oxide layer formed.

Bachmann and Munz pointed out that erroneous crack closure results could be obtained with the potential difference method, since at relatively high loads crack closure could be registered by the potential difference method which was not registered by compliance methods. This observation was probably due to the differences between 'local' and 'global' crack closure phenomena.

A major contribution to understanding crack closure was reported by Walker and Beevers[35], whose work presented the observation of a new crack-closure mechanism which occurred under plane strain conditions. They examined the crack profiles of SENT specimens of commercially pure titanium (B = 8 mm), and monitored crack mouth opening displacement. The separation of the crack faces measured by the replica technique showed a linear relation at distances greater than about 3 mm from the crack tip, but decreased rapidly and nonlinearly towards the crack tip. At $R = 0.1$ the crack appeared to remain open at minimum load, suggesting no crack closure, although the load-CMOD curve showed evidence of crack closure. Examination of the crack profile away from the crack tip, however, revealed discrete points of crack closure, generally associated with sharp deviations of the crack-growth direction. These deviations were found to be facets caused by transgranular crack growth, and the mechanism causing the contacts was thought to be a small amount of Mode II (in-plane shear) deformation. The crack closure was due therefore to the non-planar crack geometry, and the authors postulated that since it was not due to large-scale plasticity, it could occur within a specimen as well as at the edges.

Lafarie-Frenot and Gasc[36] attempted to determine the effect of localised fracture surface contact points on potential drop. Using conducting paper models of compact tension specimens they monitored potential as a simulated crack was

cut. Their results showed that localisation of crack closure greatly modified the potential drop measured, hence crack closure measured by the potential drop technique was dependent on where crack closure occurred.

Haenny and Dickson[37] used surface-mounted strain gauges (0.85 mm × 1.5 mm) as well as CMOD extensometer to measure crack closure in SEN tensile specimens (B = 12.7 mm) of 2024-T351. In agreement with the results of Bachmann and Munz[38] they observed that even at relatively high loads, the crack surfaces could remain in contact locally while globally the crack would be considered fully open. These local contact points were at the sides of the specimen, and were found to be subjected to considerable compressive stresses but to transmit negligible load. This postulate was based on the result that a higher value of crack closure load (P_{op}) was measured by the strain gauge behind the crack tip than measured by the CMOD extensometer. An examination of the curves from which the results are based indicate a questionable interpretation, however. Haenny and Dickson pointed out that the effect of contact at discrete points would decrease the potential drop measured and explain the observations of Bachmann and Munz[34].

The concept of local crack closure and global closure and their relationship was an important concept introduced by Haenny and Dickson.

Ohta *et al*[39] investigated the effect of crack closure load measurements with the position of an Elber gauge along the crack line. They used CCT specimens of high tensile strength steel (HY80). The measured value of U was found to be a minimum at the crack tip. U increased, and hence crack closure load decreased, with distance back from the tip and was a constant value at distances greater than 10 mm from the tip. They explained the result in terms of plane stress surface effects near the crack tip dominating the near-tip measurements. They suggested that for the plane-strain situation, compliance measurements remote from the crack tip may be more meaningful.

Macha *et al*[40] compared crack closure measurements made with a crack mouth displacement gauge with those determined on the surface by a laser-interferometric displacement gauge and optical interferometry. They found as did Ohta *et al* that the crack closure load was not a unique value but depended on the measurement position. For the nickel-base superalloy examined, they found from surface measurements near the crack tip that P_{op}/P_{max} was highest at the crack tip, decreasing to 5 mm from the crack tip at which the result was constant and similar to the value determined from the crack mouth displacement gauge.

Lankford and Davidson[41] attempted to circumvent the problems associated with interpreting crack closure measurements by using an SEM stereo-imaging technique. They measured the fatigue crack-tip opening displacement in 2.5mm thick SEN specimens of 7075-T6, 2024-T4 and 6061-T6 subjected to an overload cycle. The specimen was loaded in the SEM using an *in situ* servohydraulic loading stage, and the crack tip observed directly. They calculated a theoretical crack tip opening displacement (CTOD) using the estimate after Rice[42]:

$$\text{plane stress:} \quad \text{CTOD} = 0.5 \left(\frac{K}{\sigma_y}\right)^2$$

$$\text{plane strain:} \quad \text{CTOD} = 0.225 \left(\frac{K}{\sigma_y}\right)^2 .$$

To obtain a value for U ($U = (P_{max} - P_{open})/\Delta P$) they compared the measured estimate with the theoretical estimate, presumably in terms of an equivalent K value, to determine the crack closure and opening loads. Prior to an overload, they found that U_{open} *decreased with increasing alloy strength;* from 0.52 for 6061-T6 to 0.37 for 7075-T6. U_{close} was relatively constant, averaging 0.72. Following an overload, the loads required to open a crack (P_{open}) were found to steadily increase, and at the minimum crack growth rate, $U_{open} = 0.09$ and $U_{close} = 0.27$. The pre-overload measurements of crack closure indicated that for all three alloys, the value of U_{open} was smaller than would be expected from Elber's relation $U = 0.5 + 0.4R$, and was related to alloy strength. The results of Lankford and Davidson should strictly be taken as representative only of the surface behaviour, *ie* plane stress situation. Being within a vacuum would also have resulted in a higher crack tip ductility than would be the case in air, so the results may not be representative of results in air.

Bertel *et al*[43] compared crack closure measurements made using both crack mouth (CMOD) and crack tip (Elber gauge) compliance gauges. They used compact tension specimens (B = 10 mm) of 7175-T651 fatigued in air, and also investigated overload effects. They found that the total displacement range was not affected by R . They also made a distinction between crack closure at the surface and crack closure in the specimen interior, and pointed out that the compliance curve obtained at the crack tip showed two slope changes, the one at higher load indicating surface (shear lip) contact, and the transition at a lower load related to crack closure in the interior. The latter corresponded to the crack closure load

indicated by the CMOD gauge. They suggested the lower value of P_{cl} was the more meaningful, and suggested this as one factor causing confusion in the literature. They used the terminology 'local' and 'global' to differentiate between the crack closure values measured near to the crack tip and remote from it respectively. The authors concluded that Elber's assumption of a linear relationship between U and R-ratio was applicable only for the plane stress (thin sheet) situation. For thick section specimens they found a more complex dependence of U on R , due to thickness effects and the introduction of a different cracking mechanism at high R-ratios; namely a ductile dimple fracture mechanism.

Further work on 1.6mm thick CCT specimens of 2124-T351 examined R-ratio and overload effects. They confirmed Elber's relation of $U = 0.5 + 0.4R$ for thin sheet specimens. For an overload ratio of 2, a change was obtained in the crack tip compliance curve but not in the CMOD compliance curve. The results showed that only the material at the crack tip was affected by the overload, and this is not registered by the CMOD gauge. The overload effect was due mainly to crack closure effects.

2.4 Summary

A wide range of experimental techniques have been employed to study crack closure. These have involved making measurements of either 'surface' or 'bulk' effects, either by direct or indirect observation, and can be divided into the categories: mechanical (displacement); optical; ultrasonic; metallographic and electrical.

Mechanical measurement techniques have included using displacement (compliance) gauges, either at the crack mouth[44] (CMOD); or on the side faces at the crack tip, *eg* Elber (CTOD) gauge[5,20,23]; or a 'push-rod' compliance gauge[45]. The CMOD gauge technique gives a measure of 'global' crack closure, including effects due to all regions of the fracture surfaces. The method has the advantage over the CTOD gauge in that it does not have to be re-positioned during the test. Although the CTOD gauge method is purported[27] to give more accurate crack closure measurements than the CMOD gauge, it encounters possible spurious effects if positioned too close to the crack tip due to plasticity effects.

Considerable differences have also been observed between compliance techniques, especially between CTOD and CMOD results. Bertel et al[43] have suggested that the CTOD compliance curve shows two changes in slope, that at higher load being due to crack closure at shear lips and at the lower load due to crack

closure in the specimen interior. The latter they claimed coincided with the crack closure measurement determined by the CMOD gauge. Much work on crack closure has used the CTOD (Elber) gauge and this surface effect due to shear lips may explain many anomalous results with measurements made by other techniques such as the CMOD gauge. Fleck and Smith[45] developed a technique to measure crack closure within the interior of a thick specimen using a 'push-rod' displacement method. Two holes were drilled from the top of the specimen, one to below the crack plane, one to a depth just above the crack plane. A push-rod compliance gauge seated in these holes measured the crack closure in the specimen interior, which was found to be less than that observed at the specimen surface. Strain gauges have also been used to measure crack closure either mounted on the side faces near the crack line[37,46]; on the back face of compact tension specimens[46] (*ie* back face strain (BFS) method); or straddling the crack line on one surface (Schmidt gauge)[8].

The back-face-strain gauge has found widespread use, and gives a measure of 'global' crack closure. Allison *et al*[47] have compared the CMOD and BFS methods on compact tension specimens of titanium alloy, and found identical results.

The mechanical methods therefore, give 'direct' measurements of crack closure, and can measure both surface effects (Elber gauge, Schmidt gauge, side-face-strain gauge) or bulk effects (CMOD, BFS).

Optical methods have included laser interferometry[48], interferometric displacement gauge[49] and photoelastic methods using transparent plastic models[22,27]. The first two methods measure surface effects, and the latter measure bulk crack closure effects. Ray and Grandt[50] have compared three different techniques on transparent polymethyl methacrylate specimens; optical interferometry; back-face-strain (BFS) and crack mouth displacement (CMOD). The crack closure load values obtained using CMOD and BFS methods were comparable, but the crack closure loads measured along the crack front by optical interferometry were higher.

Ultrasonic methods have included the use of transmitted Rayleigh waves[10]; transmitted longitudinal waves[51]; reflected longitudinal waves[51] and diffraction and echodynamic methods[52]. Ultrasonic methods generally measure bulk effects, although focussed source methods can investigate through-thickness effects along the crack tip. Frandsen *et al*[27] have compared two ultrasonic methods; acoustic surface wave and longitudinal bulk waves with CMOD and Elber gauge results. They found some disparity between acoustic and compliance techniques. It is likely

that isolated asperity contact could show an apparently larger crack closure effect for the ultrasonic methods than for the compliance methods, which might explain the discrepancy.

Metallographic techniques have included the use of microfractography such as indirect crack closure load measurement by measuring striation markings in the SEM[53]; and direct measurements of crack closure from enlarged optical photographs of surface displacements at the crack tip[7] or *in situ* SEM examination[54]; stereo-imaging[55] and replica techniques[547]. Problems with direct observation of crack closure are mainly caused by uncertainty in determining the load where displacement ceases.

Observation of striations is a useful technique but load history effects cannot be ruled out when a programmed waveform is used, and the assumption must be made that one striation is produced per load cycle, which is a source of further uncertainty.

Electrical methods have included dc or ac potential drop techniques[9,19,21,26]. The dc method is a 'bulk' measurement technique, and the ac method is strictly a surface technique but, since it measures a through-thickness effect, it is essentially a 'bulk' measurement method.

Early work on crack closure used surface measurements on thin sheet where considerable plasticity occurred[4,5,7,23]. Lindley and Richards[21] suggested that crack closure occurred only under plane stress conditions - *ie* in slant fracture regions, and their observations were supported by photoelastic observation of PMMA[22]. Plane strain experiments using a potential drop technique on titanium[29] and on Ti-6Al-4V[19,23,24] and on aluminium alloy[56] could not be explained by contact of plane stress regions however. A complicating factor was that the PD method did not reveal much crack closure in air, but in vacuum[23,24] or dehumidified argon[19,56] crack closure was easily detected.

Irving *et al*[24] suggested that crack closure did occur in vacuum ($<10^{-5}$ mm Hz) but not in air and that water vapour increased the crack opening by modifying the strain fields near the crack tip.

Bachmann and Munz[23] proposed that crack closure was the same in both air and vacuum but in air a non-conducting layer insulated the crack faces. Both the above also measured CMOD, and again Irving detected crack closure only in vacuum, whereas Bachmann found crack closure to be independent of air pressure. The dc potential method is generally thought now to be of limited use in crack closure

studies due to the insulating effects of the oxide layer, and to 'global' crack closure effects at asperity contact points, which greatly affects PD measurements but have a limited effect on crack closure loads.

Another factor which has heightened confusion has been the terminology used by different workers. Elber[4] defined crack opening stress S_{op} and crack closure stress S_{cl} as the stresses at which the crack completely opened and completely closed on the loading and unloading half cycles respectively. It was evident, however, that below S_{op} and S_{cl} the compliance curve continued to be nonlinear before becoming linear. This indicated a progressive crack closure mechanism, which did not occur completely and suddenly at one value of applied load or stress.

Shaw and Le May[33] used different terminology which attempted to resolve this discrepancy. They called P_{op} the load at which the curve became linear, *ie* the crack was fully open (point C on Fig 2). The load at which crack closure fully ceased, *ie* when the crack was fully closed and the compliance curve again became linear (point B on Fig 2), they called P_{cl} , the crack closure load. This terminology does not seem to have become widely adopted, although the possibility exists of it being used and results published accordingly, since few researchers present their definitions of crack closure and opening loads.

Elber's definition has most widespread use, and yet the terminology of 'opening' and 'crack closure' essentially refers to the same basic mechanism, although sounding quite different in colloquial meaning. Which of these is the most important, *ie* which of these parameters influences crack growth rate has also been a point at issue, depending on which portion of the loading cycle crack growth is thought to occur, *ie* during the loading or unloading half cycle.

A particular anomaly has arisen from the fact that cracks have been observed to be wedged open remote from the crack tip by various mechanisms, so 'closure' is an inappropriate term. Beevers[57] used the term 'non-closure', which is not very satisfactory. An elegant resolution of the situation has been provided by Ritchie[58] who has recently introduced a new terminology by assigning all 'closure' phenomena to the generic term 'crack-tip shielding' mechanisms. This is a far more elegant terminology with a more obvious meaning. The implications of this terminology will be discussed in a separate section.

The majority of early work on crack closure examined 'long crack' (*ie* >5 mm) behaviour at intermediate to high ΔK values (*ie* >10 MPa$\sqrt{m}$). After 1980, a great deal of interest arose in examining other fatigue phenomena, such

as retardation due to overloads, short crack growth rate, and especially near-threshold crack growth rate. From these latter studies in particular, new crack closure mechanisms have been identified and the effect of environment has been highlighted and these aspects will be considered later. Most studies of near-threshold crack growth rate have used a load-shedding technique, in which the ΔK range at the tip of a long crack is reduced in small steps. A natural extension of this work has been to examine near-threshold crack growth rate in small cracks (1 to 5 mm) and short cracks (<1 mm). Crack closure mechanisms have also been proposed as affecting these crack growth regimes.

Crack closure arguments have, in addition, been proposed to explain or partly explain the effects of environment in all the above fatigue situations.

No attempt will be made to cover the extensive literature on all the above fatigue phenomena. Recent reviews have been published on near-threshold crack growth by Liaw[59]; and on short crack behaviour by Leis *et al*[60] and Miller[61]. Rather, particular work will be reviewed which has revealed different crack closure mechanisms for the long crack situation.

3 THE MECHANISTIC APPROACH TO CRACK CLOSURE

The second approach to investigating crack closure has been the mechanistic approach. The main fatigue crack closure mechanisms that have been identified are:

(i) plasticity induced crack closure;
(ii) roughness induced crack closure;
(iii) oxide induced crack closure;
(iv) corrosion product wedging;
(v) hydrostatic pressure induced crack closure.

The first three of these mechanisms are illustrated in Fig 4, and they will be treated in this order. Corrosion product wedging has been identified in the situation of corrosion fatigue of steel and is beyond the scope of the present survey. Hydrostatic pressure induced closure has been included for completeness but it will not be discussed, since the mechanism has been related to a viscous fluid such as oil in a crack and not to aqueous environments. A summary of the main causes of crack closure is presented in Table 1.

3.1 Plasticity-induced crack closure

Elber considered that crack closure was related to crack-tip plasticity, and caused by the residual plastic deformation left in the wake of the crack tip.

He envisaged a continuum of plasticity with the plastic zone damage merging as shown in Fig 3. This continuum model was highly effective in describing crack closure at high stresses in thin sheet material where plastic deformation was the dominant effect. This model has since been named 'plasticity induced crack closure'.

Elber[4] also noted that for his thin sheet specimens, the surfaces contacted only at discrete points or asperities on the fracture surfaces. He expressed this as 'microcompatibility' and from a rough calculation of surface area required to transmit the compressive crack closure load, concluded that the surface compatibility should be of the order of 33%.

The existence of plasticity-induced crack closure under plane strain loading has been a source of much controversy, and Fleck and Newman[62] have pointed out the conceptual difficulties of such a mechanism. Early work by Lindley and Richards[21] examined thicker section test pieces and reported that crack closure did not occur under plane strain loading mode, and that it was only the slant fracture regions (plane stress shear lips) that contacted to effect crack closure. Shaw and Le May[33] pointed out that changes in material properties or testing conditions that affected the amount of slant fracture might affect crack closure.

In addition to crack closure at slant fracture shear lips, observation of global crack closure at plastically deformed asperities has been reported by Pitoniak *et al*[22] using interferometry on PMMA (Perspex) specimens, and by Bowles[63]. The latter injected molten plastic into the tip of a closed crack and found holes in the resulting cast. These he attributed to localised crack closure at fracture surface asperities, thus preventing ingress of the plastic at these points.

Zurek *et al*[64] reported plasticity-induced crack closure in a plane strain situation when they investigated the effect of grain size on the growth rate of short cracks in 7075-T6. They used tapered cantilever beam flexural fatigue specimens, fatigued at $R = -1$ or $R = 0$ at 5 Hz in air. They monitored the length of surface cracks optically and found that short cracks grew slower in the larger grain (130 μm) material than the smaller grain (12 μm). They attributed this decrease to plasticity-induced crack closure. It is noted, however, that a similar effect of grain size reported by Scheffel *et al*[65] was explained in terms of roughness-induced crack closure, and although plasticity-induced crack closure

may have some effect, roughness-induced crack closure may have been a contributory mechanism.

Zaiken and Ritchie[66] examined the roles of local and global crack closure mechanisms in modifying crack growth rate. They observed, by machining away the crack wake of a near-threshold crack, that about 50% of crack closure was within 500 μm of the crack tip. The far-field (global) crack closure was probably due to plasticity-induced crack closure, but the near-tip crack closure they suggested was roughness-induced crack closure.

Lankford *et al*[67] attempted to rationalise differences in crack growth rate between long and short fatigue cracks. They discussed the possibility that plasticity-induced crack closure explained lower growth rates in long cracks. They found that large strains existed at the tips of short cracks which should give as much plasticity-induced crack closure as for long cracks. They appeared to confuse near tip and far-field crack closure, however, since short cracks may not experience far-field crack closure as much as long cracks.

Ritchie *et al*[68] also attempted to explain the differences in crack growth rate for large, small and surface cracks in 2124. They concurred that although other crack closure mechanisms, such as roughness induced crack closure, were probably operative at near-threshold levels, the differences in the results for the various crack geometries were largely due to different amounts of crack tip shielding in the wake of the crack tip.

Up until 1980, virtually all crack closure was measured on long fatigue cracks and was ascribed to plasticity-induced crack closure. This included crack closure due to macroplasticity effects (shear lips) under plane stress conditions as well as microplasticity effects at the crack tip and in the crack wake under plane strain loading conditions. Mathematical models such as proposed by Newman[69,70] and Budiansky and Hutchinson[71] assumed the model of localised plasticity at the crack tip. Work on overload effects also utilised plasticity-induced crack closure mechanisms which appeared to explain the overload situation.

There have been disagreements about where fracture surface contact is occurring due to plasticity-induced crack closure. Elber[4] observed that crack closure could occur at discrete points well away from the crack tip (presumably observed within shear lips). Lindley and Richards[21] observed crack closure within the shear lips, and this relates to the macroplasticity situation.

Pitoniak *et al*[22] observed crack closure in thick section within shear lips and within the centre (plane strain) region at discrete points. Crack closure has generally been considered to decrease progressively back from the crack tip, and mathematical models have assumed a plasticity continuum and have incorporated a simple progressive crack closure contribution. Asperity or shear lip contact mechanisms have not, however, been considered. Plasticity-induced crack closure therefore, includes both crack closure due to macroplasticity - *ie* shear lips, as well as microplasticity occurring under plane-strain conditions at intermediate to high ΔK values. The latter crack closure may occur very close to the crack tip, or at asperities remote from the crack tip, or both. The terminology was improved when in 1980 Haenney and Dickson[37] introduced the terminology of 'local' and 'global' components of crack closure. The relative effects of these two components on reducing the crack tip stress intensity was investigated by Zaiken and Ritchie[66] among others. The general consensus of opinion is that generally, global (or far-field) crack closure has a significant but not a dominant effect, whereas crack closure at the crack tip (near-field) has a dominant effect. Crack closure due to shear lips is a complicating factor that may be included in either of these. A more satisfactory terminology to distinguish various phenomena contributing to crack closure is that of 'crack tip shielding' which is described later.

The role of plasticity-induced crack closure on crack growth rate in conditions of low ΔK values has been considered by some workers.

Newman[70] carried out a computer simulation for crack closure which indicated that the sharp decrease in crack growth rates near threshold were due to residual plastic deformation well back from the crack tip which reduced the crack tip loading. He concluded that the threshold might be an artificial entity, being simply a reflection of the residual plastic deformation.

Minakawa *et al*[72] attempted to determine the role of far-field (global) crack closure on near-threshold crack growth rate during a K-decreasing test. They machined away the wake of a fatigue crack in a 6.3mm thick compact tension specimen of aluminium alloy X7090-T6 prepared by powder metallurgy. A crack was grown under ΔK decreasing conditions, crack closure was measured by a crack mouth compliance gauge, and crack wake was removed by electro-discharge machining. Removal of the wake did result in a higher crack growth rate for a limited growth increment, and crack closure level was reduced. They concluded that the far-field (global) crack closure was not the reason for the observation

of a crack-growth threshold but did have a modifying effect. Important crack closure events also took place within 1 mm of the crack tip, and they concluded that near-tip crack closure was predominant.

A large number of workers have used plasticity-induced crack closure arguments to explain fatigue crack growth rate retardation due to an overload. Among these are Sharpe and Grandt, and Ward-Close and Ritchie.

Sharpe and Grandt[48] used a laser interferometry technique on 2024-T851 specimens to measure crack opening displacements, *ie* the load at which the crack faces completely separated. They found that following an overload, the stress intensity factor at which the faces separated, K_{open} , was increased thus reducing the ΔK range. This reduction in ΔK explained the crack-growth retardation.

Ward-Close and Ritchie[73] investigated overload behaviour in an α/β type titanium alloy, IMI 550, using both near-tip surface strain gauges and CMOD displacement gauge. They found that the initial acceleration in crack growth rate following an overload was due to an immediate reduction in near-tip crack closure and a slight decrease in far-field crack closure. Subsequent retardation was not associated with changes in far-field crack closure, but indications of an increase of up to 50% in near-tip crack closure were observed, which, if verified, would explain the crack-growth rate retardation.

3.2 Roughness-induced crack closure

The first workers to observe a crack closure mechanism other than plasticity-induced crack closure were Walker and Beevers[35], who examined two-stage surface replicas of crack profiles in 8mm thick SEN specimens of α-titanium. They observed that at low ΔK values (near threshold) and low R-ratio, the crack faces were separated at minimum load due to localised contact at discrete points on the fracture surfaces. They found that these contact regions were associated with sharp deviations in the crack-growth direction from normal to the tensile axis, and they related the degree of crack deviation to microstructure, and mode of crack growth. Deviation of the crack path was caused by transcrystalline facet formation in favourably oriented grains, and the displacement responsible for causing contact at discrete points they suggested was a small amount of Mode II (in-plane shear) deformation.

A number of workers have investigated near-threshold crack growth and shown that crack behaviour is different from that at higher stress intensities. Near-threshold crack growth has been found to be associated with increased sensitivity

to stress history[74], material mechanical properties[74,75], load ratio[76,77] and microstructural variation[78]. Cooke and Beevers[75] found that as ΔK was reduced towards threshold, the effect of R increased, and K_{max} became rate controlling at low ΔK values.

A new fatigue fracture mechanism unique to low crack growth rates was reported by Cooke and Beevers[75] and by Birkbeck *et al*[79] in steels and in titanium by Robinson *et al*[83]. They reported a crystallographic fracture mode at low ΔK values.

Minakawa and McEvily[80] proposed an elegant rationale to explain the different crack closure mechanisms observed at low and high ΔK values. Their explanation was based upon the different crack-growth modes observed in the different ΔK regimes, and they supported their hypothesis by citing the observations of several other workers.

Otsuka *et al*[81] had observed different fracture surface crack growth morphologies in low carbon steel. At low ΔK values, they observed a faceted morphology indicative of a shear mode crack growth mechanism. At higher ΔK values they observed a ductile striated morphology indicative of tensile mode crack growth. These fracture morphologies they noted were analogous to those designated by Forsyth[82] as Stage I and Stage II fatigue crack-growth regimes. Forsyth reported that in Stage I the crack initiates and propagates in a surface slip band which is operative due to shear stress. In Stage II crack growth, the crack propagates perpendicular to the principal tensile stress. The major difference between these two stages is that in Stage I there is one primary slip system active parallel to the direction of crack growth with a component of tensile stress acting perpendicular to this direction, *ie* a combination of Mode I (tensile opening) and Mode II (in-plane shear). When the crack changes to Stage II growth, propagating perpendicular to the principal tensile stress, the crack growth occurs under Mode I loading, and in this mode at least two slip systems must act at an angle to the direction of crack growth in order for the crack to open and blunt in each loading cycle.

Minakawa and McEvily[80] explained that crack advance by slip on a single-slip system can lead to fracture surface mismatch, as illustrated in Fig 5. The role of the Mode I component was suggested as giving rise to irreversible plastic deformation which resulted in crack advance.

Roughness-induced crack closure results therefore from slip planarity leading to a faceted crack morphology, and is predominant when the 'roughness' of the surface is of the same order as the crack opening displacement.

A number of workers investigated the effects of metallurgical variables on near-threshold crack-growth rate.

Ritchie and Suresh[3] considered the effects of grain size on crack closure in the near-threshold growth regime. They considered the results due to Asaro *et al*[83] on fine and coarse grained (d = 63 μm and 190 μm respectively) aluminium alloy 2048-T851 and explained the increase in crack closure measured by a roughness induced crack-closure mechanism.

Carter *et al*[84] investigated the effects of ageing condition, grain size and environment on crack-growth rate. Compact tension (B = 7.1 mm) specimens were tested at $R = 0.1$, $f = 30$ Hz in environments of laboratory air (RH 50%) and vacuum (10^{-6} torr). Crack closure was measured using a displacement gauge. In air, fatigue crack-growth rates plotted as da/dN vs ΔK_{eff} were similar for all grain sizes and ageing conditions. In vacuum, however, large differences were seen, and generally the underaged conditions showed lower growth rates than the overaged conditions. Grain size had a more marked effect on the growth rates of the underaged materials. The authors found that the crack profile of the underaged material showed extreme non-planarity, whereas the crack profile of the overaged material was planar. They explained the effects of grain size in terms of increased crack closure stresses due to roughness induced crack closure. The improved fatigue resistance in vacuum they explained by increased slip reversibility and absence of embrittlement by moisture.

Lafarie-Frerot and Gasc[85] found a dependence of roughness induced crack closure on ageing condition in 7075 aluminium alloy. Comparing underaged and hyperoveraged conditions, crack closure due to surface roughness was greater in the underaged alloy in which planar slip predominated.

Scheffel *et al*[65] also found that the extent of roughness induced crack closure was controlled partly by grain size. The extent of crack closure was found to increase with increase in grain size, especially at low R in Al-Mg-Si alloy and in 7075. They also found crack closure in coarse grained Al-Zn-Mg-1.5Cu but not in fine grained (fibrous) 7075. Grain size was not the only parameter influencing crack closure, however. Specimen type was also a factor, the more compliant specimen (CT) having a value of K_{op} twice that for the same material in a clamped SEN bend specimen. This agreed with McEvily[86] who suggested that

roughness induced crack closure caused by contributions from non-Mode I deformations might be more pronounced in more compliant (*eg* CT) than stiffer (SENT or CCT) specimens.

Suresh and Ritchie[87] proposed a 'geometric model' to estimate the dependence of crack closure on degree of surface roughness. Assuming the surface to comprise identical 'triangular waveform' profiles, they related the mismatch gap (COD) due to crack closure, to the height of surface features, and defined a nondimensional surface roughness parameter, γ . This simple model predicted increased crack closure with increased surface roughness, and they proposed from the model that reduction of near-threshold crack growth rates with increased grain size or lower material strength could be explained by the increased crack closure due to roughness-induced crack closure effects.

Roughness-induced crack closure is generally used to describe contact of faceted fracture features which are dimensionally small, *eg* of the order of the grain size. There are situations, however, where crack closure can occur due to macroscopic crack branching/meandering or crack deflection. Venkateswara Rao *et al*[88] for example reported significant crack deflection in the aluminium-lithium alloy 2090-T8E41. The crack tip is thought to be 'shielded' from the full ΔK range and hence there is some degree of crack closure as proposed by Ritchie[89]. Whether this is due to a contact crack closure mechanism, an asperity contact mechanism, or to the decreased stress intensity factor due to nonplanarity, or a combination of the three is open to debate. The latter mechanism has been treated by Cotterell and Rice[90] who produced a solution for a simply kinked crack and showed that the crack driving force was significantly reduced compared to a crack oriented at 90° to the tensile axis, under pure Mode I loading. The implications of crack deflection in the short and long crack situations has received some attention from Suresh[91]. Ritchie[89] has discussed crack deflection as a crack tip shielding mechanism separate from other 'contact' crack closure phenomena, and this will be discussed later.

3.3 Oxide-induced crack closure

The formation of oxide debris on fatigue fracture surfaces has been known since the early work on fretting fatigue. Tomlinson *et al*[92] observed that fretting which produced oxide debris occurred between two metallic surfaces brought into repeated frictional contact in air. They observed that the phenomenon occurred even under very small relative displacements (±1.3 *nm*) at low loads and small number of cycles (*eg* 100). The effect was found to be greater if one

surface was polished, and was dependent upon the hardness of the two materials and the hardness of the oxide formed.

The effect of an oxide layer in the context of crack closure was first observed as affecting the crack closure measurements obtained by the electric potential method. Irving *et al*[9] for example failed to observe crack closure for titanium in air using the pd method but observed crack closure in vacuum. The explanation generally held was that an electrically insulating oxide layer formed in air which prevented the detection of crack closure by the pd method.

Cooke and Beevers[93] reported the observation of an oxide layer on pearlitic C-Mn steel in near-threshold fatigue tests. The rust-like corrosion product was not observed during fatigue at intermediate ΔK values, but only under decreasing K conditions. The density of corrosion product was observed to decrease when the R-ratio was increased from 0.05 to 0.8. Near-threshold crack growth rates were found to be markedly affected by R-ratio, with a threshold value of 12 $MPa\sqrt{m}$ at $R = 0.05$ and 4 $MPa\sqrt{m}$ at $R = 0.72$.

The first workers to suggest that oxidation or corrosion products could produce crack closure were Paris *et al*[76]. They investigated the effects of R-ratio and temperature on crack growth rates and threshold values of two steels in air and distilled water. Threshold values in air were decreased by increasing R-ratio and this stress ratio dependence decreased with increasing temperature. The greatest sensitivity to temperature occurred at threshold, and was less for higher R-ratios. Near-threshold crack-growth rates were found to be lower in distilled water than in air. They explained their results in distilled water in terms of corrosion product contributing to crack closure. It is noted that the temperature effect they reported could also be explained by an oxide-induced crack closure mechanism.

Bachmann and Munz[38] noted that the amount of oxide on a fracture surface could be increased by an oxide formation/destruction mechanism during repeated contact of the fracture surfaces.

An extensive study of surface oxidation was carried out by Benoit *et al*[94]. They studied the oxidation of the fatigue fracture surface of austenitic stainless steel (AISI 316) at low crack-growth rates. Threshold fatigue tests under decreasing ΔK conditions produced bands of different coloured oxide on the fracture surfaces, and they analysed the oxide layer to determine if the colours were caused by differences in oxide thickness or type. In air, the coloured bands represented a particular growth rate, and the thickness of the film was found to

be inversely proportional to the crack-growth rate. In vacuum, however, they observed a uniform oxide layer thickness. In air, oxide layer thickness was constant under constant ΔP loading, but under decreasing ΔP (threshold) testing the oxide layer thickness increased markedly. They also attempted to measure any temperature rise at the crack tip which might account for the oxide formation, but were unsuccessful. They suggested a mechanism involving the oxidation of slip steps emerging at the crack tip. They termed the oxidation process 'fretting oxidation' and postulated that the mechanism was a form of fretting corrosion, involving adhesion (friction welding) followed by decohesion (tearing of oxide layer or shearing of welded regions).

Another possible cause of oxide formation derives from the work of Attermo and Ostberg[95], who observed a temperature rise of up to 14°C at the tip of a fatigue crack in stainless steel. Highest temperatures were recorded at longer crack lengths and hence when crack tip plasticity was extensive ($R = 0.1$). This mechanism does not seem to be applicable to near-threshold conditions however, where crack tip plasticity is generally thought to be limited. It is noted, however, that Lankford and Davidson[67] have proposed a mechanism of intense, highly localised plasticity at the tip of a low ΔK near-threshold crack which might give credence to an effect of temperature on oxide formation.

An effect of oxide formation upon crack growth by a crack closure mechanism was also proposed by Ritchie *et al*[96]. They measured near-threshold fatigue crack propagation rates in 2¼Cr-1Mo pressure vessel steel, at $R = 0.05$ to 0.8 in moist air, dry hydrogen gas and dry argon gas. They used a 12.7mm thick compact tension test piece and measured threshold (ΔK_0) under both decreasing and increasing ΔK conditions. In moist air environment, crack-growth rates at intermediate ΔK values were not altered by changing R-ratio, but at low ΔK values (<10 MPa$\sqrt{m}$) increasing R-ratio led to a marked decrease in the threshold, ΔK_0 . The threshold value for $R = 0.3$ (7 MPa$\sqrt{m}$) was between the value for $R = 0.05$ (9 MPa$\sqrt{m}$) and $R = 0.5$ and $R = 0.8$, the latter two showing a similar threshold value of 5 MPa$\sqrt{m}$. In dry hydrogen, all R-ratios above $R = 0.05$ gave a similar crack growth behaviour and threshold value of around ΔK_0 4.5 MPa$\sqrt{m}$, lower than in air, and at $R = 0.05$ a value of 7 MPa$\sqrt{m}$, again lower than that observed in air. Ritchie *et al* explained the results not in the usual terms of a hydrogen-embrittlement mechanism which accelerated the crack growth rate in hydrogen, but rather in terms of an oxide-induced crack closure mechanism which reduced the growth rate in air. The result was verified by testing in a dry argon atmosphere, which showed similar growth rates to those observed in dry

hydrogen. The higher growth rates in dry gaseous environment were therefore due to reduced oxide-induced crack closure than that produced in a moist environment.

Stewart[97] also observed the reduction in ΔK_0 due to dry gaseous environments compared to moist air. He also observed oxide debris which he termed 'fretting oxide' and on the fracture surfaces of low alloy steels he used, found it to consist of α and $\gamma - Fe_2O_3$. In common with Ritchie *et al*[96] he observed that the moist environment only affected near-threshold crack-growth rate, and was more marked at lower R values. He too explained his results in terms of an increase in crack closure due to fretting oxide. No environmental effect on ΔK_0 was observed for the higher strength steel, which he explained by the smaller plastic zones in higher strength material hence reducing crack closure effects. Also, fretting by hard oxide particles would be reduced in the higher strength material. Stewart proposed that oxide was formed by fretting of plastically deformed material at the tip of the crack. The magnitude of crack closure, he proposed, could be calculated from the reduction in crack-tip opening displacement (CTOD) resulting from fretting oxide build-up. Using the equation

$$\text{CTOD} = \frac{K^2(1 - \upsilon^2)}{2E\sigma_y} ,$$

where σ_y = yield stress, E is Young's modulus and γ is Poisson's ratio. He calculated an approximate value of CTOD = 0.2 μm , and observed oxide particles of up to 3 μm thick on the fracture surface which indicated that oxide particles could affect crack closure at low values of ΔK .

To explain the observation that no fretting oxide or environmental effect in moist air was observed at intermediate crack growth rates, Stewart suggested that plasticity induced crack closure due to shear lips might come into play which prevented the centre of the specimen from closing (as observed by Lindley and Richards[21]) which would prevent oxide formation by a fretting mechanism.

Suresh *et al*[98] used an oxide induced crack closure argument to explain the effect of moist environments on near-threshold crack-growth rates in bainitic and martensitic 2¼Cr-1Mo steels. Tested at low ΔK in moist air, the fracture surface showed a band of oxide at low R-ratio (0.05) but not at high R-ratio (0.75). They favoured the mechanism proposed by Benoit *et al*[94] of repeated breaking and compaction of the oxide at the crack tip (fretting oxidation). Measuring oxide layer thickness, they found that the oxide layer thickness was a

maximum at the threshold, was significantly smaller in hydrogen gas compared to air at $R = 0.05$, and was an order of magnitude lower in either environment at $R = 0.75$. The thickness of oxide layer was significantly greater than that observed from exposing bare metal to the environment for the same length of time.

Liaw *et al*[99] examined near-threshold behaviour in electrolytic tough pitch (ETP) copper using specimens of thickness: 6.35 mm (WOL); 9.0 mm (CT); 6.35 mm (CCT). They found that increasing the R-ratio led to significantly increased threshold crack-growth rates. Also, that the R-ratio effect was reduced by increasing material strength - annealed copper showed a higher value of ΔK_o than full-hard material at low R-ratio. They interpreted their results by a fretting oxide crack closure mechanism as proposed previously, observing that increased Mode II crack opening occurred at near-threshold loading which would produce fretting. Also, a rise in crack-tip temperature would increase oxide formation. Their results were in agreement with those of Ritchie *et al*[96] and Stewart[97].

Oxide-induced crack closure appears to be a significant crack closure mechanism only when the thickness of the oxide layer is of the same order of magnitude as the crack-tip opening displacement (CTOD). This situation is most likely to exist at near-threshold crack-growth rates. Under these conditions, additional factors exist to favour oxide formation, such as increased Mode II displacements and very slow crack growth hence a large number of cycles per crack-growth increment which would favour a fretting oxidation mechanism.

The role of Mode II deformation has been suggested in regard to fretting fatigue and this highlights the point that crack closure produced by any mechanism, such as plasticity-induced or roughness-induced, results in increased fretting oxidation at the crack tip. Oxidation-induced crack closure may therefore, be a contributing factor to another crack closure mechanism. This aspect was demonstrated by Tokaji *et al*[100] who investigated the effects of sheet thickness on near-threshold crack growth in low carbon and high-strength steels in moist air. Oxide was more obvious visually on the low carbon steel, indicating a dependence on material strength/hardness or grain size/microstructure. Both steels showed a dependence of threshold on sheet thickness, decreasing from $B = 2$ mm down to a minimum at $B = 8$ mm, then increasing, the thickness effect being more pronounced in the low carbon steel. They attributed the dependence of near-threshold crack-growth characteristics on sheet thickness for $B > 8$ mm to oxide-induced crack closure promoted by asperities on fracture surfaces or

roughness-induced crack closure. The higher threshold values (greater resistance to crack growth) observed for thinner sheet specimens down to 2 mm they attributed to mixed mode displacements.

This work effectively demonstrated the interdependence of oxide-induced crack closure on other crack closure mechanisms, and also the secondary dependence on material and specimen geometry parameters.

3.4 Crack tip shielding

Elber[4] proposed that the crack tip would close as plastically deformed material at the crack tip contacted upon unloading. He envisaged that the contact would progressively occur away from the crack tip as the load was decreased further, below the crack closure load, P_{cl} . Lindley and Richards[21] showed that for the situation of plane stress and plane strain, the crack tip in the plane strain (tensile fracture) region could be propped open by the contact of the plane stress (slant fracture) shear lips. The term 'crack closure' was appropriate for the regions contacting in the shear lips, but not quite so apt for the plane strain region if the crack remained open.

Further difficulties in terminology arose when the crack tip was found to be wedged open by a roughness-induced crack closure mechanism[35]. Contact, or crack closure, occurred at discrete points and not necessarily at the crack tip. Beevers and Halliday[57] recognised the unsuitability of the term crack closure when the crack tip was wedged open, and suggested the term 'non-closure'. This terminology was, however, inherently ambiguous.

Ritchie[58] has proposed a solution in terms of defining the concept of 'crack tip shielding'.

It is a concept which circumvents many of the misleading terminology associated with crack closure and embraces a range of phenomena under one generic term.

The concept is based upon the principle that a crack is driven by the presence of a 'crack driving force' and opposed by the resistance of the microstructure. The crack driving force may be characterised by the stress intensity parameter, K , and crack advance is restrained by 'toughening' the material. Ritchie divides toughening mechanisms into two classes: intrinsic, *ie* by increasing the inherent microstructural resistance to crack advance; and extrinsic, *ie* crack advance is impeded by other phenomena such as crack closure. He further subdivides the extrinsic toughening mechanisms into four categories:

(i) Crack deflection and meandering.

(ii) Zone shielding.

(iii) Contact shielding.

(iv) Combined zone and contact shielding.

These categories are illustrated schematically in Fig 6.

Under combined zone and contact shielding, Ritchie includes plasticity-induced crack closure. Under contact shielding, he includes crack closure phenomena that wedge the crack open, such as roughness-induced crack closure, and corrosion-debris-induced crack closure.

4 MODELLING CRACK CLOSURE

Elber[5] presented the first attempt to quantify crack closure. He first defined an effective stress ratio, ΔS_{eff} , where

$$\Delta S_{eff} = S_{max} - S_{op} .$$

He then defined an effective stress range ratio, U , where

$$U = \frac{S_{max} - S_{op}}{S_{max} \cdot S_{min}} = \frac{\Delta S_{eff}}{\Delta S} .$$

Plotting experimental data for 2024-T3 material, he found a linear relationship between U and R ;

$$U = 0.5 + 0.4R \qquad (-0.1 < R < 0.7) \qquad (1)$$

where $R = S_{min}/S_{max}$.

The stress intensity factor range, ΔK would be modified by crack closure to an 'effective' value, ΔK_{eff} , where $\Delta K_{eff} = U.\Delta K$.

The relationship for crack-growth rate due to Paris and Erdogan[2] which states:

$$\frac{da}{dN} = C(\Delta K)^n ,$$

where C and n are constants.

Elber re-wrote in terms of ΔK_{eff} as follows:

$$\frac{da}{dN} = C\left[(0.5 + 0.4R)\Delta K\right]^n$$

for 2024-T3, $C = 1.21 \times 10^{-9}$ and $n = 3.62$.

Schijve[101] found that Elber's equation correctly predicted the trends for $R > 0$, but was unrealistic at $R < 0$. By defining the parameter γ , where

$$\gamma = \frac{S_{op}}{S_{max}} ,$$

hence $\gamma = 1 - (1 - R)U$.

He wrote Elber's equation as

$$\gamma = 0.5 + 0.1R + 0.4R^2 \quad . \tag{2}$$

Newman's analytical work[69] had shown that as $R \rightarrow -1$ it was unlikely that U would rise, and Schijve proposed the following expression, derived from experimental data:

$$U = 0.55 + 0.35R + 0.1R^2 \quad , \tag{3}$$

hence

$$\gamma = 0.45 + 0.2R + 0.25R^2 + 0.1R^3 \quad .$$

To make the expression more flexible he introduced the factor α :

$$U = 0.55 + (0.45 - \alpha)R + \alpha R^2 \tag{4}$$

and hence

$$\gamma = 0.45 + (0.1 + \alpha)R + (0.45 - 2\alpha)R^2 + \alpha R^3 \quad .$$

The expression is plotted in Fig 7a for various values of α . Good correlation of experimental data tested at various R-ratios was obtained using equation (4) and $\alpha = 0.12$.

De Konig[102] proposed a relation for γ from experimental results on 7075-T6, as follows:

$$\gamma = 0.45 + 0.2R - 0.15R^2 + 0.9R^3 - 0.4R^4 \qquad \text{for } R > 0$$

$$\gamma = 0.45 + 0.2R \qquad \text{for } R \leq 0 .$$

Bachmann and Munz[23] proposed an expression from experimental data on titanium which took into account the maximum stress intensity factor:

$$U = \frac{1}{1 - R}\left[1 - \frac{6.67R}{K_{max}} - \frac{4.27}{K_{max}}\right].$$

Katcher and Kaplan[20] proposed the expression based on experimental data;

$$U = 0.68 + 0.91R \qquad \text{for } 0.08 < R < 0.32 .$$

Notable attempts to model crack closure analytically have been made by Newman.

Newman[69] attempted to calculate the crack closure using a finite element analysis method. He modelled a centre-cracked panel using a model composed of two-dimensional constant-strain triangular elements of unit thickness, and for the crack-tip region used three different mesh sizes. The panel material was assumed to have a yield stress (σ_0) of 350 MPa and a modulus of elasticity (ε) of 70 GPa. For constant amplitude loading (R = 0) with maximum gross stress S_{max} of $0.4\sigma_0$. The crack-closure stress stabilized after the eighth loading cycle at about 75% of S_{max} , and appeared to be governed by the maximum strain reached on the crack-tip element prior to crack extension. The crack-opening stress was found to stabilize after five cycles at about 50% of S_{max} , which was in good agreement with Elber's measurements[5]. For $R = 0.5$ and $S_{max} = 0.4\sigma_0$, the crack-opening stress stabilized at about 68% of S_{max} , which was about 5% higher than that measured by Elber[5]. For $R = -1$ and $S_{max} = 0.3\sigma_0$, the crack-opening stress was lower than for $R = 0$, implying that compression stresses caused yielding of the contacting surfaces. The effect of R-ratio is summarised in

Fig 7b. [Note: Newman's nomenclature - the crack closure stress, $S_{c\ell}$, is the stress at which crack closure occurs on *unloading*, whereas S_{op} is the stress at which crack closure ceases to occur during loading.]

Newman[70] carried out a further analysis based upon a three-dimensional boundary element model of crack growth for plane strain and plane stress situations. He used a Dugdale strip-yield model modified to leave plastically deformed material in the wake of the advancing crack. The model calculated crack opening stress as a function of R for constant amplitude loading, and incorporated a constraint factor, α , to simulate the plane stress ($\alpha = 1$) and plane strain ($\alpha = 3$) situations. Newman's results are shown in Fig 8a plotted as S_0/S_{max} (*ie* effective R-ratio) against R . For R-ratios less than $R = 0.6$, crack closure is significantly higher for the plane stress situation than the plane strain situation. The results also showed that the position of the curve for negative R-ratio was dependent upon the ratio σ_{max}/σ_y .

The model also predicted that only near the crack tip are significant loads transmitted across the crack faces, and the material near the crack tip was found to yield in compression.

Budiansky and Hutchinson[71] modelled crack closure in a two-dimensional Mode I crack based on the assumption of small-scale yielding according to the ideally-plastic Dugdale-Barenblatt model. This model applies only to plane-stress conditions. They concluded that crack closure would be expected to occur and that an effective stress intensity range ΔK_{eff} was an appropriate parameter to use. They considered also the effect of cyclic hardening and found that cyclic hardening increased crack closure, while cyclic softening alleviated crack closure effects.

Marissen *et al*[103] investigated the effects of compression loads on crack closure and crack-growth rate. They used a mathematical model to estimate the wedge stresses and determined an expression for K_{op}/K_{max} for negative R values as follows:

$$\frac{K_{op}}{K_{max}} = 0.5\left(1 - \left(\frac{S_c}{S_{yc}}\right)^2\right),$$

where S_c = compression stress

S_{yc} = yield stress in compression.

They accepted that Elber's equation was an acceptable fit for R values ≥ 0 . Their equation showed reasonably good agreement with Schijve's formula for $\alpha = 0.12$ and with Newman[75] for S_{min} values of $\frac{1}{3}S_{yc}$.

All the analytical models described so far have modelled plasticity-induced crack closure. With the discovery of other forms of crack closure, some workers have used a broader analytical approach. This has been based upon the 'crack tip shielding' concept proposed by Ritchie[89].

Beevers *et al*[104] defined a stress intensity value which acts upon the crack tip as soon as asperities come into contact. This they called $K_I(local)$, and they then developed a mathematical model for local crack closure. Their assumption was that the crack-tip stress intensity factor was a superposition of local and global contributions as follows:

$$K_I = K_I(local) + K_I(global) .$$

A two-dimensional single asperity model was developed. The model showed that the height of the asperity, its distance from the crack tip and its rigidity could significantly influence the crack-closure stress intensity. The model showed reasonable agreement between predicted and observed behaviour for microstructural asperities in nickel alloys and oxide asperities in steels.

$$K_I(local) = \left(\frac{2}{\pi(C + R_p)}\right)^{\frac{1}{2}} \left| \frac{1}{Eb} + \frac{2}{\pi GL} (1 - \upsilon) \right|^{-1}$$

$$K_I(global) = \frac{LG}{2(1 - \upsilon)} \left(\frac{2\pi}{C + R_p}\right)^{\frac{1}{2}} .$$

where C = distance from asperity to crack tip
R_p = plastic zone radius
G = rigidity modulus
L = asperity height
γ = Poisson's ratio
E = Young's modulus.

Buck *et al*[105] considered the role of asperity contact in crack-tip shielding. They calculated a crack-tip shielding stress intensity factor at each individual asperity contact given by

$$K_i = \frac{2^{1/2}}{(\pi d)^{3/2}} P_i \frac{1}{1 + (z/d)^2} ,$$

where d = nearest distance between the contact and crack tip

P_i = load carried by the individual contact

z = coordinate along the crack front with its origin at the closest point of the contact.

Superposition of the SIFs of a series of contact points gave the expression

$$dK_{sh} = \left(\frac{2}{\pi}\right)^{1/2} \frac{\Delta P}{B d^{1/2}} .$$

Buck *et al*[51] also presented a treatment similar to that of Beevers *et al*[104] for separating the influence of local and global crack closure on the stress intensity factor, K. These components they termed K_I(local) and K_I(global), and the instantaneous stress intensity factor (SIF) was therefore the sum of these components:

$$SIF = K_I(local) + K_I(global) .$$

They proposed that even in the unloaded condition, if the crack tip is wedged open, there would still be a SIF, *ie* K_I(local) acting upon the crack tip.

K_I(local) thus 'shielded' the crack tip from experiencing the full crack driving force, ΔK, defined as

$$\Delta K = K_{Imax}(global) - K_{Imin}(global) .$$

They proposed therefore, that the crack tip would experience a driving force given by:

$$\Delta K_{eff} = K_{Imax}(global) - K_{Imax}(local) .$$

It is now standard procedure to define ΔK_{eff} as:

$$\Delta K_{eff} = K_{Imax}(global) - K_{Iclosure}$$

or

$$\Delta K_{eff} = K_{Imax}(global) - K_{Iopening} .$$

5 THE EFFECT OF AN AQUEOUS LIQUID ENVIRONMENT ON CRACK CLOSURE

Much work has been carried out to measure crack closure in different gaseous environments, but the effect of a liquid environments has received limited attention. Early work compared inert and moisture containing environments and showed that the more inert the environment the greater the plasticity involved in crack propagation. Buck *et al*[106] for example used an acoustic surface wave technique to investigate the effects of environment on crack closure in part-through-crack (PTC) specimens of 7075-T651. A reasonably clearly defined crack closure point was observed in air of 15% RH and 80% RH, but in dry nitrogen the crack closure was not well defined, with evidence of limited crack closure throughout the loading cycle. The crack closure load appeared to be lowest in air 80% RH, higher in air 15% RH and highest in dry nitrogen. Fractography revealed different fracture surface features for the three environments: transgranular at 80% RH; flat featureless facets with striations at 15% RH; and ductile rough surface features in dry nitrogen. They concluded therefore, that there was a correlation between fracture surface ductility and crack closure stress. They further postulated that the ductility of the material in the plastic zone was reduced by a dislocation-oxygen interaction.

More recently, Carter *et al*[84] have investigated the effects of air and vacuum on crack closure in underaged and overaged 7475 alloy in large and small grain size conditions. They found that the most fatigue resistant condition in laboratory air was the coarse-grained underaged condition, which they explained in terms of increased crack closure due to greater surface roughness. The lowest growth rates were observed in vacuum, which they explained by the absence of environmental embrittlement and ease of slip reversibility. Similar crack closure was attributed to contact of surface asperities. A large grain size did not give the expected increase in crack closure in vacuum as in air, which they attributed to the reversibility of Mode II displacement in vacuum.

Work in gaseous environments has suggested therefore, that crack-tip plasticity, and hence crack closure, can be affected by the environment. Much environmental work has also brought to light the effects of oxide layers in producing increased crack closure. This aspect has been considered in detail in section 3.1.

The first observations of crack closure mechanisms affecting corrosion fatigue crack growth derived from testing of steels in aggressive media. The effects of more aggressive environments on crack growth resulting from crack closure were first reported for steels fatigue in salt water. In 1969, Endo *et al*[107] observed a reduced crack growth rate in rotating steel specimens tested in salt water and they explained the cause as 'wedge action caused by the metal oxide in cracks, which reduced the strain amplitude at the crack tip', (an observation made, incidentally, before Elbers elucidation of crack closure). A number of workers have since confirmed these and similar observations, such as van der Velder *et al*[108]. These workers observed fatigue crack retardation in structural steels tested in artificial seawater, and were aware that many previous observations of retardation had been explained by crack branching and crack blunting mechanisms. They found, however, that crack growth retardation was associated with and explained by an increased crack closure load level. The formation of a thick oxide layer on the fracture surfaces indicated that corrosion product wedging was the mechanism responsible for enhanced crack crack closure and hence crack growth retardation.

Clerivet and Bathias[109] appear to have been the first workers to systematically investigate the effects of a liquid environment on crack closure. They examined 7175-T651 aluminium alloy in air and salt water, fatigued at 10 Hz in air and 0.2 Hz in salt water, $R = 0.01$ and $R = 0.5$. Using 10 mm thick compact tension specimens they measured crack closure using both crack-mouth and crack-tip (surface) compliance methods. They found that the salt water environment reduced the crack-opening displacement (COD) at both P_{min} and P_{max} compared to air, but that the COD range was not affected. Comparing the load-displacement plots from the crack mouth (CMOD) and crack tip (CTOD) the crack closure point from the CTOD gauge was much higher than that measured by the CMOD gauge. They explained the higher crack closure load as surface crack closure (contact of shear lips) and the lower value as 'inside' crack closure in the interior of the crack. The correlation is shown in Fig 9.

The salt water environment produced slightly higher values of crack-mouth displacement at P_{max} at $R = 0.1$ and slightly higher values at P_{min} at $R = 0.5$. When salt water was introduced into a fatigue crack growing in air,

however, the crack-mouth displacements for both P_{min} and P_{max} were observed to decrease immediately. After a number of cycles in salt water, the displacements tended to exceed those in air. It is noted that this latter observation could be due simply to the change in compliance with crack extension unless constant ΔK testing was employed, which is not stated. They postulated that 'inside' crack closure loads were slightly higher in salt water than in air.

Ewalds[110] measured crack closure at the crack tip on the surface of 2024-T3 CCT specimens (B = 6 mm), using a displacement gauge. The specimens were thinned in consecutive steps of 0.4 mm after which the crack closure load was again measured. Fatigue tests were carried out in vacuum (10 Hz) air and salt water (1 Hz), and all crack closure measurements were carried out in air. They detected a variation in crack opening stress S_{op} along the crack front, being lower in the specimen interior than at the surface. They concluded that S_{op} was not affected by environment. The width of shear lips was, however, affected by environment, and was much reduced by salt water. They argued that crack closure was not affected by environment, hence the plastic zone size was similar for different environments. They conceded, however, that the microplasticity directly at the crack tip may be affected by environment. They also postulated from their results that there was no correlation between plastic zone size and shear lip width. In addition, they investigated the effect of specimen thickness on crack closure by thinning the specimen in increments of 0.4 mm and measuring the crack closure load. The clip gauge was positioned 1 mm behind the crack tip (in air), and crack closure load was found to vary along the crack front as the specimen interior was penetrated. Closure was found to be higher at the surface and lower in the specimen interior, in accordance with the work of Lindley and Richards[21]. The work does, however, show a serious anomaly in that crack growth rates measured in air and salt water were similar, which is not in accord with other workers and casts doubt on the validity of their conclusions.

Further work by Ewalds *et al*[111] measured fatigue crack growth rates for 2024-T3 in air, demineralised water, oxygenated and deoxygenated salt water. They chose load ratios ranging from $R = -1$ to $R = 0.33$, and a test frequency of 10 Hz. These workers made no measurements of crack closure, but plotted their data with an effective stress intensity factor range calculated using the equations for U presented by Elber[5] and Schijve[101].

The results in air at different R-ratios were reasonably well in agreement when plotted using Elber's formula, and in extremely good agreement using Schijve's formula. In the aqueous environments the results showed fairly poor

agreement using Elber's formula, but good agreement using Schijve's formula. The discrepancies they put down to the influence of corrosion product wedging, and concluded that environment had no effect on crack closure load. The work is limited in its general applicability, however, mainly by the use of a relatively high test frequency (10 Hz) at which corrosion fatigue effects may be absent or limited, and also by the use of quite low R-ratios (up to $R = 0.33$). Using higher R-ratios may have shown a more marked effect of environment using their correlation technique.

The R-ratio effect on crack growth rate might show indirectly some effect of environment on crack closure. Comparative data is, however, scarce but some data have been published in an ESDU handbook[112] for 7475-T761 in air and sump tank water, for $R = 0.1$ and $R = 0.5$ at $f = 13$ Hz . The curves in each environment were approximately parallel and the effects of R-ratio appeared to be independent of environment, except for a slightly greater effect at higher crack growth rates in air and a greater effect at low growth rates in sump water. Again, the relatively high frequency of 13 Hz may have limited the effect of the corrosive environment.

Shih and Wei[113] carried out tests to determine the effect of R-ratio on crack growth rate in 2219-T851 exposed to water vapour. They found that crack growth rate in an inert environment increased with increasing R-ratio for a given value of ΔK , as would be expected. Crack growth rate was found to be dependent upon water vapour pressure up to a 'saturation' value above which no further crack growth enhancement occurred. For pressures above 'saturation' value, crack growth rate was independent of R-ratio. They concluded that the effects of load ratio on environment assisted fatigue crack growth could be attributed to two sources - one relating to its effect on local deformation at the crack tip (mechanical component) and the other on its role in modifying gas transport (corrosion fatigue component).

Bathias[114] compared the effect of R-ratio on crack growth rates for 2618A-T651 and 7175-T7351 in argon, wet air and salt water. He examined centre-cracked specimens of thickness 1.6 mm and 10 mm at $R = 0.01$ and $R = 0.5$ at a test frequency of 1 Hz. In all cases in an inert environment the growth rate curves for high and low R-ratio were parallel for all values of ΔK . This was not always the case, however, for the wet air and salt water curves. In all cases, the effect of aqueous environment was more marked at the lower R-ratio. The environmental effect was generally more pronounced at lower ΔK values, especially at low R-ratio. For the 7175-T7351 material tested in salt water, comparing the

effect of R-ratio showed that at low ΔK values, the R-ratio effect was small - the curves converging. The divergence at higher ΔK values is not easy to explain in terms of restriction of flow of environment to the crack tip. Using closure arguments, these results could be interpreted as indicating that in an aggressive environment, crack closure is increasing at higher ΔK values. The certain conclusion that can be drawn from these data is that the R-ratio effect is environmentally dependent in these two alloys, being more pronounced in the 7175-T7351 material.

Suresh *et al*[115] tested alloy 2021-T6 in dry hydrogen, moist air, distilled water and hydrazine environments to investigate if oxide-induced crack closure might reduce the crack growth rate. They found significant increases in crack growth rate in both distilled water and hydrazine environments. Near-threshold behaviour was similar in all the environments, and an analysis of the fracture for moist air and distilled water showed an oxide layer thickness of 100-250A. They concluded that oxide-induced crack closure did not occur in this alloy to affect crack growth rates.

Since enhanced crack closure occurs after an overload, investigations into overload situations in an aggressive environment might give some insights into the effect of environment on crack closure.

Zuidema *et al*[116] tested 6 mm thick CCT specimens of 2024-T351 in air and seawater under constant ΔK loading. After application of an overload, they measured the delay, and found that seawater could either increase or decrease the delay. They explained the results in terms of a balance between the increase in delay due to corrosion product wedging, and the increase in crack growth rate due to corrosion fatigue. A corrosion product wedging mechanism was supported by investigation of the oxide layer on the fracture surfaces fatigued in salt water, which were found to be up to 15 times thicker than those formed in air. Their conclusions, however, were not very convincing and lacked experimental support.

Wei *et al*[117] also examined the effect of salt water on overload behaviour, for alloy 2219-T851. They found that the delay due to an overload (*ie* the overload affected zone) was dependent upon specimen thickness, on K_{max} , and was independent of environment.

Bathias[114] compared crack growth rates in 2618A-T651 and 7175-T7351 in dry argon, humid air and salt water. The effect of changing R-ratio from $R = 0.01$ to $R = 0.05$ was found to give a greater reduction in crack growth rate in the inert environments. This effect was more marked in the lower strength alloy

2618A-T651. Measuring crack closure on 7175-T651 using a displacement gauge, he reported that the displacement at maximum load was slightly higher in salt water than in air. The stress intensity value at which crack closure occurred was slightly higher in salt water than in air, hence ΔK_{eff} was higher by about 1.5 MPa$\sqrt{m}$ in air than in salt water, for all crack lengths.

A further factor which might be relevant to corrosion fatigue testing in liquid environments was the discovery by Tzou *et al*[118] of closure caused by hydrodynamic wedging. These workers investigated the effects of dehumidified silicone and paraffin oils of different viscosities on fatigue crack growth in bainitic steel. Growth rates at $R = 0.05$ in the near-threshold regime were higher than those in moist air by up to a factor of two. Behaviour at $R = 0.75$ was the same in the two environments. Furthermore, crack growth rates tended to increase with increasing oil viscosity. They explained the complex dependence of crack growth rate in dry oils in terms of three mutually competitive mechanisms: (a) suppression of moisture-related corrosion fatigue processes; (b) minimization of oxide-induced crack closure; and (c) development of additional closure through a hydrodynamic action caused by penetration of the oil inside the crack.

Raizenne *et al*[119] have investigated the effects of inert (dry argon) and salt water atmospheres on fatigue crack growth rate and crack closure in 7475-T7351 and 7091-T7E78. Tests were performed on 12.7 mm thick CT specimens at R-ratios of 0.1 and 0.5 at a test frequency of 20 Hz. Crack closure was observed in 7475-T7351 for $R = 0.1$ in both argon and salt water, and the effects were similar. At $R = 0.5$, a small effect of closure was observed in salt water and not in argon. The finer grained powder metallurgy alloy 7091-T7E78 however, showed quite different results. No closure was observed in argon, but in salt water, considerable crack closure was observed at $R = 0.1$. The authors concluded that the larger grained 7475-T7351 material exhibited roughness induced closure which was not significantly affected by a salt water environment. The 7091-T7E78 material did not show any closure in argon, but considerable closure in salt water, which they attributed to oxide layer build up due to corrosion. The results indicate that any differences in crack closure due to environment were only observable below a ΔK value of 10 MPa$\sqrt{m}$.

6 CONCLUSIONS

This literature survey has shown that there is an overwhelming weight of evidence to support the postulate that crack closure can play a major role in influencing the fatigue crack growth rate. The previous uncertainties have been

shown to be related to differences in experimental measurement or analysis techniques. In order to produce meaningful data, it is evident that extreme care must be exercised in the choice of measurement technique for the experimental set-up in question. The data obtained must also be analysed with care, and it must be established whether the technique employed measures surface or though-thickness closure, and whether it measures local or global crack closure effects, or both.

Ultrasonic and optical techniques have been shown to have specialised applications and the electrical potential drop methods have generally been shown to have limited use. The most reliable and unambiguous data appear to be achieved by the use of compliance techniques.

Test piece thickness has been a major experimental variable which can affect the crack closure mechanism. A thin test piece in which the crack tip experiences considerable plasticity usually exhibits plasticity-induced crack closure. In thick test pieces however, plasticity-induced crack closure has not been found to play a major role except in shear-lip regions, although roughness-induced and oxide-induced crack closure can have a marked effect.

The role of crack closure has been shown to be dependent upon a number of factors such as alloy strength, grain structure, crack morphology, loading conditions and environment. A comparison of crack growth rates cannot therefore, assume a similar level of crack closure in the variants unless crack closure has been measured and incorporated accordingly. Crack closure may significantly affect the fatigue crack growth rate in-service, and crack growth rate may be accelerated or retarded by a change in the service conditions. In order to quantify and understand this situation, crack closure effects should be investigated and taken into account.

Table 1

SUMMARY OF THE CAUSES AND OCCURRENCE OF THE MAIN CRACK CLOSURE MECHANISMS

Crack closure mechanism	Cause	Major occurrence
Plasticity-induced crack closure	Residual plastic deformation in the wake of the crack tip (cyclic plasticity)	Long crack: intermediate to high ΔK ranges. In air, and especially in vacuum
Roughness-induced crack closure	Small-scale branching and deflection of the crack path, and Mode II crack opening component	Near-threshold crack growth, *ie* low ΔK where crystallographic Stage I crack growth occurring
Oxide-induced crack closure	Wedging action due to fretting oxidation in gaseous environment, usually moist air	Generally observed for long crack at near-threshold stresses in moist air, large number of applied fatigue cycles
Corrosion debris-induced crack closure	Wedging action due to corrosion products produced in aqueous environments	During corrosion fatigue in aggressive environment, *eg* steel in sea water aluminium alloys in sea water

REFERENCES

No.	Author	Title, etc
1	Irwin, G.R.	*Applied Mat. Res.*, **3**, p 65 (1964)
2	Paris, P.C. Erdogan, F.	*Trans. ASME*, Series **D4**, pp 528-534, December 1963
3	Ritchie, R.O. Suresh, S.	*Met. Trans.*, **13A**, pp 937-940 (1982)
4	Elber, W.	*Eng. Fract. Mech.*, **2**, 1, pp 37-45 (1970)
5	Elber, W.	in 'Damage tolerance in aircraft structures'. ASTM STP 486, American Society for Testing & Materials, Philadelphia PA, pp 230-242 (1971)
6	Cheng, Y.F. Brunner, N.	*Int. J. Fract. Mech.*, **6**, pp 431-434 (1970)
7	Adams, N.J.I.	*Eng. Fract. Mech.*, **4**, pp 543-554 (1972)
8	Roberts, R. Schmidt, R.A.	*Int. J. Fract. Mech.*, **8**, pp 469-471 (1972)
9	Irving, P.E. Robinson, J.L. Beevers, C.J.	*Int. J. Fract.*, **9**, pp 105-108 (1973)
10	Buck, O.	*Int. J. Fract.*, **8**, pp 121-124 (1972)
11	Buck, O. Ho, C.L. Marcus, H.L.	*Eng. Fract. Mech.*, **5**, pp 23-34 (1973)
12	Bucci, R.J. Paris, P.C.	*J. Mater.*, **7**, p 402 (1972)
13	Hertzberg, R.W. von Euw, E.F.J.	*Met. Trans.*, **4**, pp 887-889 (1973)
14	Bates, R.C. Clark, W.G.	*Trans. ASM*, **62**, pp 380-389 (1969)
15	Ritchie, R.O. Knott, J.F.	*Acta Met.*, **21**, pp 639-648 (1973)

REFERENCES (continued)

No.	Author	Title, etc
16	Hudson, C.M. Scardina, J.T.	*Eng. Fract. Mech.*, **1**, pp 429-446 (1969)
17	Frost, N.E. Pook, L.P. Dorton, K.	*Eng. Fract. Mech.*, **3**, pp 109-126 (1971)
18	Pearson, S.	*Eng. Fract. Mech.*, **4**, pp 9-24 (1972)
19	Shih, T.T. Wei, R.P.	*Eng. Fract. Mech.*, **6**, pp 19-32 (1974)
20	Katcher, M. Kaplan, M.	in 'Fracture toughness and slow stable cracking'. ASTM STP 559, American Society for Testing & Materials, Philadelphia PA, p 264-282 (1974)
21	Lindley, T.C. Richards, C.E.	*Mat. Sci. Engng.*, **14**, pp 281-293 (1974)
22	Pitoniak, F.J. *et al*	*Eng. Fract. Mech.*, **6**, pp 663-670 (1974)
23	Bachmann, V. Munz, D.	*Int. J. Fract.*, **11**, pp 713-716 (1975)
24	Irving, P.E. Robinson, J.L. Beevers, C.J.	*Int. J. Fract.*, **11**, pp 1055-1056 (1975)
25	Ritchie, R.O. Knott, J.F.	*Acta. Met.*, **21**, pp 639-648 (1973)
26	Irving, P.E. Robinson, J.L. Beevers, C.J.	*Eng. Fract. Mech.*, **7**, pp 619-630 (1975)
27	Frandsen, J.D. Inman, R.V. Buck, O.	*Int. J. Fract.*, **11**, pp 345-348 (1975)

REFERENCES (continued)

No.	Author	Title, etc
28	Gomez, M.P. Ernst, H. Vazquez, J.	*Int. J. Fract.*, **12**, pp 178-180 (1976)
29	Shih, T.T. Wei, R.P.	*Int. J. Fract*, **13**, pp 105-106 (1977)
30	Clarke, C.K. Cassatt, G.C.	*Eng. Fract. Mech.*, **9**, pp 675-688 (1977)
31	Garrett, G.G. Knott, J.F.	*Int. J. Fract.*, **13**, pp 101-108 (1977)
32	Garrett, G.G. Knott, J.F.	*Met. Trans.*, **7A**, pp 884-886 (1976)
33	Shaw, W.J.D. LeMay, I.	in 'Fracture mechanics'. ASTM STP 677, American Society for Testing & Materials, Philadelphia PA, pp 233-246 (1979)
34	Bachmann, V. Munz, D.	*Eng. Fract. Mech.*, **11**, pp 61-71
35	Walker, N. Beevers, C.J.	*Fat. Eng. Mat. Str.*, **1**, pp 135-148 (1979)
36	Lafarie-Frenot, M.C. Gasc, C.	*Int. J. Fract.*, **15**, pp R121-R123 (1979)
37	Haenny, L. Dickson, J.I.	*Int. J. Fract.*, **16**, pp R121-R125 (1980)
38	Bachmann, V. Munz, D.	*Eng. Fract. Mech.*, **11**, pp 61-71 (1979)
39	Ohta, A. Kosugee, M. Sasaki, E.	*Int. J. Fract.*, **11**, pp R53-R57 (1979)
40	Macha, D.E. *et al*	*Exp. Mech.*, **19**, pp 207-213 (1979)

REFERENCES (continued)

No.	Author	Title, etc
41	Lankford, J. Davidson, D.L.	in '*Proc. 5th Int. Conf. on Fracture, Advances in Fracture Research*', Cannes, France, **2**, pp 899-906 (1981)
42	Rice, J.R.	in 'Mechanics of crack tip deformation and extension by fatigue: Fatigue crack propagation'. ASTM STP 415, American Society for Testing & Materials, Philadelphia PA, p 247 (1967)
43	Bertel, J.D. Clerivet, A.	in '*Proc. 5th Int. Conf. on Fracture, Advances in Fracture Research*', Cannes, France, **2**, pp 943-951 (1981)
44	Carman, C.D. Turner, C.C. Hillberry, B.M.	in 'Mechanics of fatigue crack closure'. ASTM STP 982, J.C. Newman & W. Elber Eds., American Society for Testing & Materials, Philadelphia, pp 214-221 (1988)
45	Fleck, N.A. Smith, R.A.	*Int. J. Fatigue*, **4**, 3, pp 157-160 (1982)
46	Ward-Close, C.M. Ritchie, R.O.	in 'Mechanics of fatigue crack closure'. ASTM STP 982, J.C. Newman & W. Elber Eds., American Society for Testing & Materials, Philadelphia, pp 93-111 (1988)
47	Allison, J.E. Ku, R.C. Pompetzki, M.A.	IBID, pp 171-185 (1988)
48	Sharpe, W.N. Grandt, A.F.	in 'Mechanics of crack growth'. ASTM STP 590, American Society for Testing & Materials, Philadelphia, pp 302-320 (1976)
49	Donahue, R.J. *et al*	*Int. J. Fract. Mech.*, **8**, 2, pp 209-219 (1972)
50	Ray, S.K. Grandt, A.F.	in 'Mechanics of fatigue crack closure'. ASTM STP 982, J.C. Newman & W. Elber Eds., American Society for Testing & Materials, Philadelphia, pp 197-213 (1988)

REFERENCES (continued)

No.	Author	Title, etc
51	Buck, O. Rehbein, D.K. Thompson, R.B.	*Eng. Fract. Mech.*, **28**, pp 413-424 (1987)
52	Bouami, D. DeVadder, D.	*Eng. Fract. Mech.*, **23**, pp 913-920 (1986)
53	Sunder, R. Dash, P.K.	*Int. J. Fatigue*, **4**, pp 97-105 (1982)
54	Davidson, D.L.	in 'Mechanics of fatigue crack closure'. ASTM STP 982, J.C. Newman & W. Elber Eds., American Society for Testing & Materials, Philadelphia, pp 44-61 (1988)
55	Williams, D.R. Davidson, D.L. Lankford, J.	*Exp. Mech.*, **20**, pp 134-139 (1980)
56	Unangst, K.D. Shih, T.T. Wei, R.P.	*Eng. Fract. Mech.*, **19**, pp 725-734 (1977)
57	Beevers, C.J. Halliday, M.D.	*Int. J. Fract.*, **15**, pp R27-R30 (1979)
58	Ritchie, R.O.	*Mat. Sci. Eng.*, **A103**, pp 15-28 (1988)
59	Liaw, P.K.	in 'Mechanics of fatigue crack closure'. ASTM STP 982, J.C. Newman & W. Elber Eds., American Society for Testing & Materials, Philadelphia, pp 62-92 (1988)
60	Leis, B.N. *et al*	*Eng. Fract. Mech.*, **23**, 5, pp 883-898 (1986)
61	Miller, K.J.	*Fat. Eng. Mater. Struct.*, **10**, 2, pp 93-113 (1987)
62	Fleck, N.A. Newman, J.C.	in 'Mechanics of fatigue crack closure'. ASTM STP 982, J.C. Newman & W. Elber Eds., American Society for Testing & Materials, Philadelphia, pp 319-341 (1988)

REFERENCES (continued)

No.	Author	Title, etc
63	Bowles, C.Q.	The role of environment, frequency and wave shape during fatigue crack growth in aluminium alloys. Delft University of Technology, The Netherlands, Report LR-270, May 1978
64	Zurek, A.K. James, M.R. Morris, W.L.	Met. Trans., **14A**, pp 1697-1705 (1983)
65	Scheffel, R. Ibas, O. Detert, K.	*Proc. 3rd Int. Conf. on fatigue and fatigue thresholds*, Charlottesville, Virginia (Fatigue 1987), **1**, pp 155-164, June 1987
66	Zaiken, E. Ritchie, R.O.	*Met. Trans.*, **16A**, pp 1467-1477 (1985)
67	Lankford, J. Davidson, D.L. Chan, K.S.	*Met. Trans.*, **15A**, pp 1579-1588 (1984)
68	Ritchi , R.O. *et al*	*Fat. Fract. Eng. Mater. Struct.*, **10**, pp 343-362 (1987)
69	Newman, J.C.	in 'Mechanics of crack growth'. ASTM STP 590, American Society for Testing & Materials, Pennsylvania PA, pp 281-301 (1976)
70	Newman, J.C.	ASTM STP 748, American Society for Testing & Materials, Pennsylvania PA, pp 53-84 (1981)
71	Budiansky, B. Hutchinson, J.W.	*J. Appl. Mech.*, **45**, pp 267-276 (1978)
72	Minakawa, K. Newman, J.C. McEvily, A.J.	*Fatigue Engng. Mat. Str.*, **6**, pp 359-363 (1983)
73	Ward-Close, M.W.C. Ritchie, R.O.	in 'Mechanics of fatigue crack closure'. ASTM STP 982, American Society for Testing & Materials, Philadelphia PA, pp 93-111 (1988)

REFERENCES (continued)

No.	Author	Title, etc
74	Klesnil, M. Lukas, P.	*Eng. Fract. Mech.*, **4**, pp 77-92 (1972)
75	Cooke, R.J. Beevers, C.J.	*Mat. Sci. Eng.*, **13**, pp 201-210 (1974)
76	Paris, P.C. et al	in 'Stress analysis and growth of cracks'. ASTM STP 513, American Society for Testing & Materials, Philadelphia PA, pp 141-176 (1971)
77	Bucci, R.J. Clark, W.G. Paris, P.C.	IBID, pp 177-195
78	Robinson, J.L. Beevers, C.J.	*Met. Sci. J.*, **7**, pp 153-159 (1973)
79	Birkbeck, G. Inckle, A.E. Waldron, E.W.J.	*J. Mater. Sci.*, **6**, pp 319-323 (1971)
80	Minakawa, K. McEvily, A.J.	*Scripta. Met.*, **15**, pp 633-636 (1981)
81	Otsuka, A. Mori, K. Miyata, T.	*Eng. Fract. Mech.*, **7**, pp 429-439 (1975)
82	Forsyth, P.J.E.	*Acta. Met.*, **11**, p 703 (1963)
83	Asaro, R.J. Hermann, L. Baik, J.M.	*Met. Trans.*, **12A**, pp 1133-1135 (1981)
84	Carter, R.D. et al	*Met. Trans.*, **15A**, pp 555-572 (1984)
85	Lafarie-Frenot, M.C. Gasc, C.	*Proc. Int. Conf. on 'Advances in fracture research'*. (ICF6) New Delhi, India, **3**, pp 2041-2048 (1984)

REFERENCES (continued)

No.	Author	Title, etc
86	McEvily, A.J.	*Met. Sci.*, **11**, pp 274-284 (1977)
87	Suresh, S. Ritchie, R.O.	*Met. Trans.*, **13A**, pp 1627-1631 (1982)
88	Venkateswara Rao, K.T. Yu, W. Ritchie, R.O.	*Met. Trans.*, **19A**, pp 549-561 (1988)
89	Ritchie, R.O.	*Mat. Sci. Eng.*, **A103**, pp 15-28 (1988)
90	Cotterell, B. Rice, J.R.	*Int. J. Fract.*, **16**, pp 155-169 (1980)
91	Suresh, S.	*Met. Trans.*, **14A**, pp 2375-2385 (1983)
92	Tomlinson, G.A. Thorpe, P.L. Gough, H.J.	*Proc. Inst. Mech. Eng.*, London, **141**, p 223 (1939)
93	Cooke, R.J. Beevers, C.J.	*Mat. Sci. Eng.*, **13**, pp 201-210 (1974)
94	Benoit, D. Namdar-Tixier, R. Tixier, R.	*Mat. Sci. Eng.*, **45**, pp 1-8 (1980)
95	Attermo, R. Ostberg, G.	*Int. J. Fract. Mech.*, **7**, pp 122-124 (1971)
96	Ritchie, R.O. Suresh, S. Moss, C.M.	*J. Eng. Mat. Tech. Trans. ASME (H)*, **102**, pp 293-299 (1980)
97	Stewart, A.T.	*Eng. Fract. Mech.*, **13**, pp 463-478 (1980)
98	Suresh, S. Zamiski, G.F. Ritchie, R.O.	*Met. Trans.*, **12A**, pp 1435-1443 (1981)
99	Liaw, P.K. *et al*	*Met. Trans*, **13A**, pp 1607-1618 (1982)

REFERENCES (continued)

No.	Author	Title, etc
100	Tokaji, K. Ando, Z. Nagae, K.	*J. Eng. Mat. Tech.*, **109**, pp 86-91 (1987)
101	Schijve, J.	*Eng. Fract. Mech.*, **14**, pp 461-465 (1981)
102	de Konig, A.U.	A simple crack closure model for prediction of fatigue crack growth rates under variable amplitude loading. NLR Report MP 80006 (1980)
103	Marissen, R. Trautmann, K.H. Nowack, H.	*Eng. Fract. Mech.*, **19**, pp 863-879 (1984)
104	Beevers, C.J. *et al*	*Eng. Fract. Mech.*, **19**, pp 93-100 (1984)
105	Buck, O. Thompson, R.B. Rehbein, O.K	*Mat. Sci. Eng.*, **A103**, pp 37-42 (1988)
106	Buck, O. Fransen, J.D. Marcus, H.L.	*Eng. Fract. Mech.*, **7**, pp 167-171 (1975)
107	Endo, K. Komai, K. Ohnishi, K.	*Memorandum of Faculty of Engineering*, Kyoto University, **31**, pp 25-46 (1969)
108	van der Velder, R. *et al*	in 'Corrosion fatigue: Mechanics, metallurgy, electrochemistry and engineering'. American Society for Testing & Materials, Pennyslvania PA, pp 64-80 (1983)
109	Clerivet, A. Bathias, C.	*Eng. Fract. Mech.*, **12**, pp 599-611 (1979)
110	Ewalds, H.L.	*Eng. Fract. Mech.*, **13**, pp 1001-1007 (1980)

REFERENCES (concluded)

No.	Author	Title, etc
111	Ewalds, H.L. van Doorn, F.C. Sloof, W.G.	in 'Corrosion fatigue: Mechanics, metallurgy, electrochemistry and engineering'. ASTM STP 801, pp 115-134 (1983)
112	Engineering Sciences Data Unit	*Fatigue and fracture mechanics data*, **2**, Item 88007, p 85, June 1988
113	Shih, T.T. Wei, R.P.	Eng. Fract. Mech., **18**, pp 827-837 (1983)
114	Bathias, C.	in 'Corrosion fatigue of aircraft materials'. AGARD R-659, Advisory Group for Aerospace Research & Development, April 1977
115	Suresh, S. Palmer, I.G. Lewis, R.E.	*Fat. Eng. Mat. Struct.*, **5**, pp 133-150 (1982)
116	Zuidema, J. Mense, P.J.M. Edwards, R.A.H.	*Eng. Fract. Mech.*, **26**, pp 927-935 (1987)
117	Wei, R.P. *et al*	*J. Eng. Mat. Tech.*, **102**, pp 280-292 (1980)
118	Tzou, J.L. Suresh, S. Ritchie, R.O.	*Acta Met.*, **33**, pp 117-127 (1985)
119	Raizenne, M.D. *et al*	in 'New materials and fatigue resistance aircraft design'. Proc. 14th ICAF, Ottawa, Canada, Ed. D.L. Simpson Publ. EMAS UK, pp 177-194 (1987)

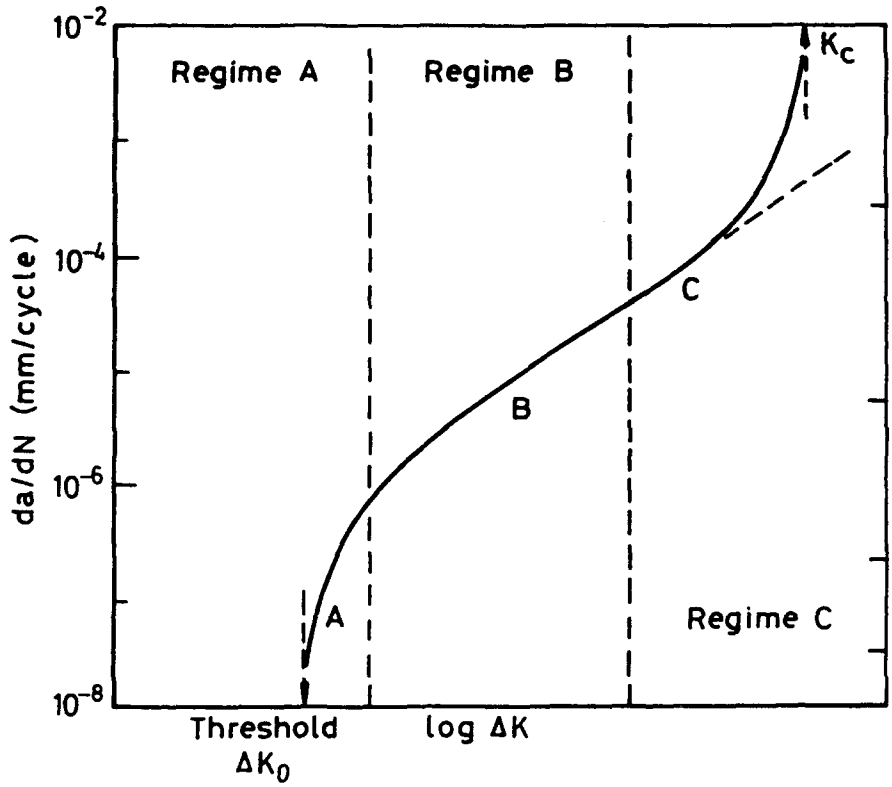

Fig 1 Generalised fatigue crack growth rate curve showing the three major crack growth regimes, after Ritchie[3]

Fig 2

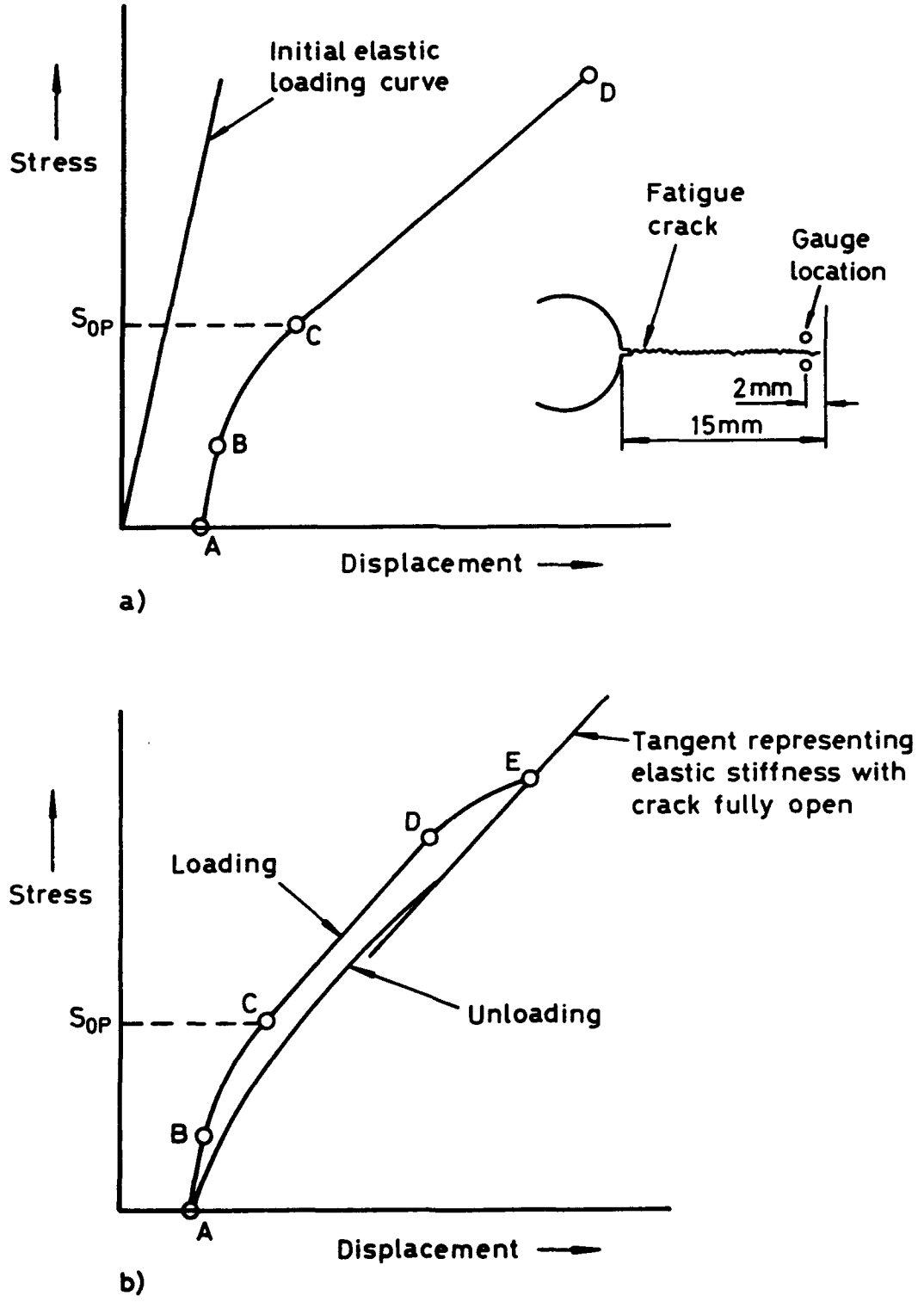

Fig 2 Illustration of the stress-displacement behaviour observed (a) with gauge 2 mm from crack tip; (b) with gauge situated at the crack tip (exaggerated for clarity), after Elber[5]

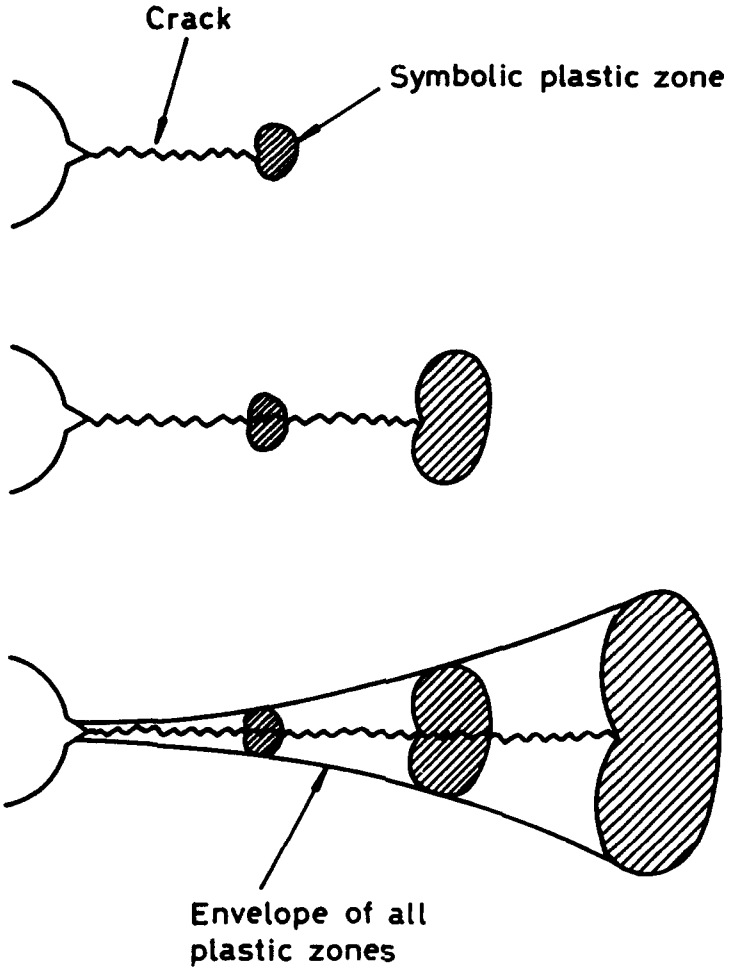

Fig 3 Development of a plastic zone envelope around a fatigue crack, after Elber[5]

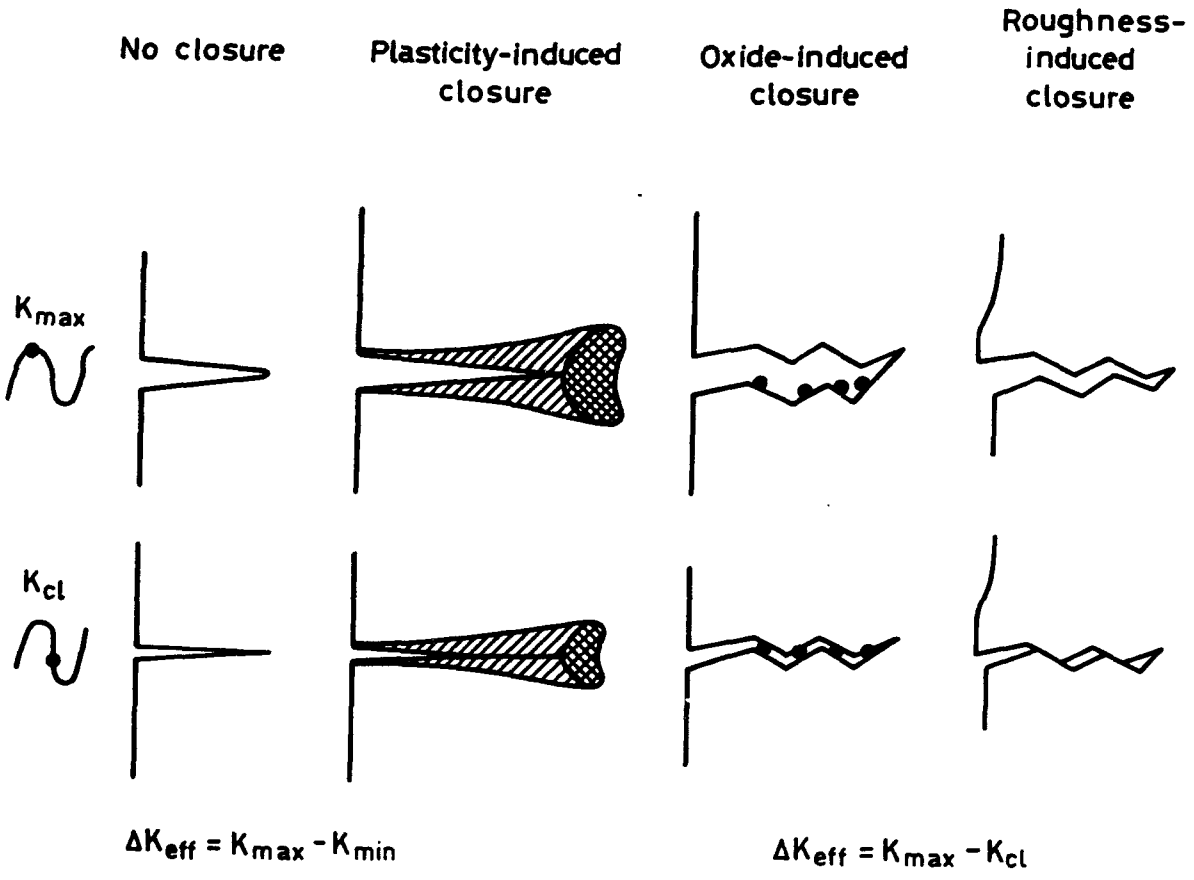

Fig 4 Schematic illustration of the main mechanisms of fatigue crack closure, after Suresh and Ritchie[87]

Fig 5

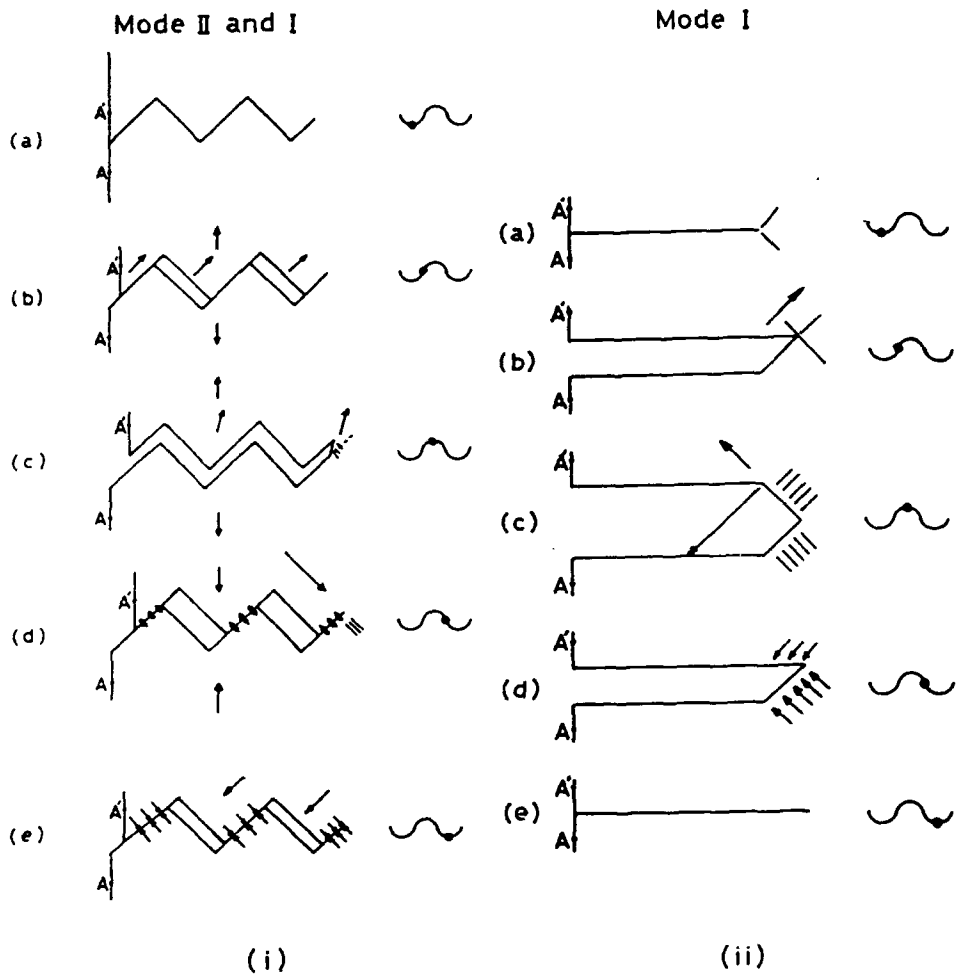

Fig 5 Schematic illustration of fatigue crack growth under (i) combined Mode I and Mode II loading; and (ii) under Mode I loading only, after Minakawa[80]

Extrinsic toughening mechanisms

1 Crack deflection and meandering

2 Zone shielding

- transformation toughening
- microcrack toughening
- crack wake plasticity
- crack field void formation
- residual stress fields
- crack tip dislocation shielding

3 *Contact shielding*

- wedging:
  - corrosion debris-induced crack closure
  - crack surface roughness-induced closure
- bridging:
  - ligament or fibre toughening
- sliding:
  - sliding crack surface interference
- wedging + bridging:
  - fluid pressure-induced crack closure

4 Combined zone and contact shielding

- plasticity-induced crack closure
- phase transformation-induced closure

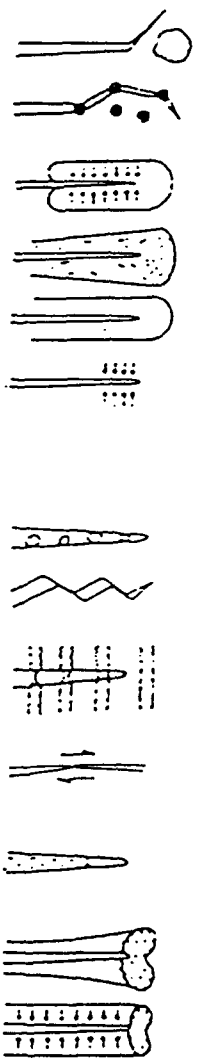

Fig 6 Schematic illustration of crack tip shielding mechanisms, after Ritchie[58]

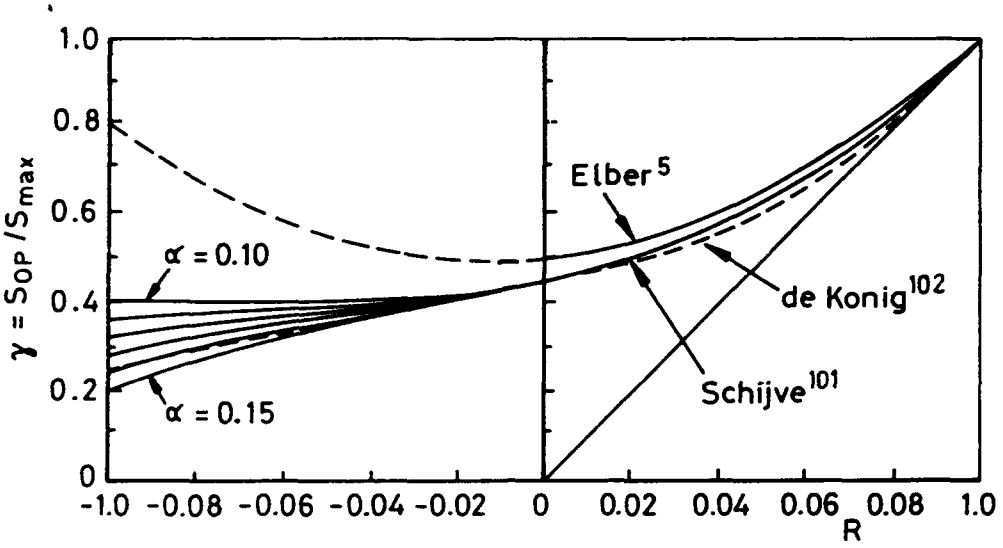

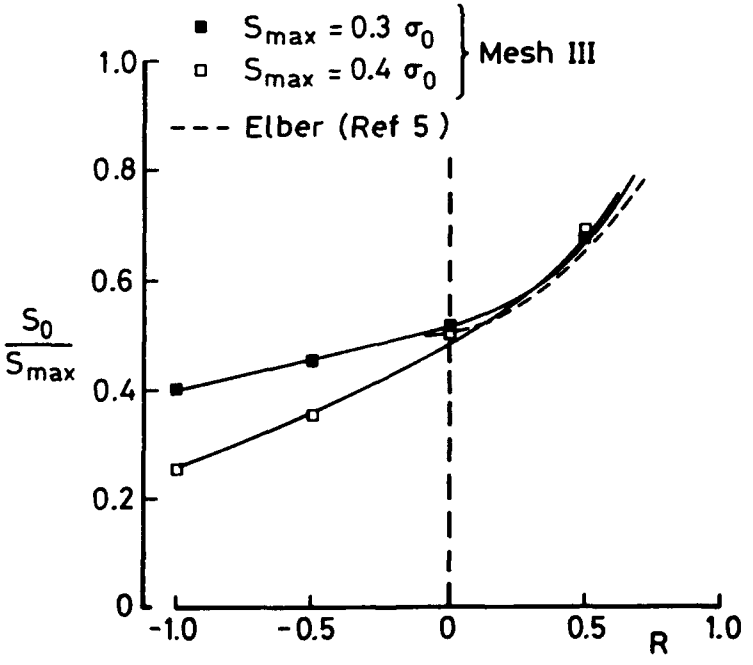

TR 90046

Fig 7 (a) Plots of S_{op}/S_{max} calculated by Schijve[101]; (b) Plots of crack opening stress calculated by Newman[69] compared with Elber[5] experimental data

Fig 8a&8b

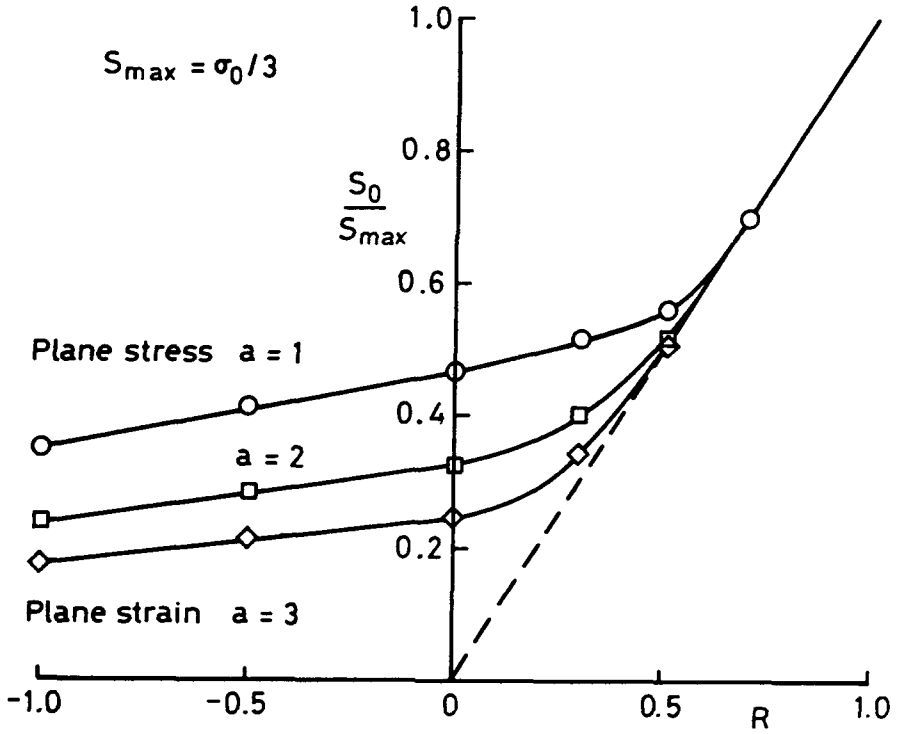

Fig 8a Normalised crack-opening stress as a function of R-ratio for simulated plane-stress and plane-strain conditions after Newman[70]

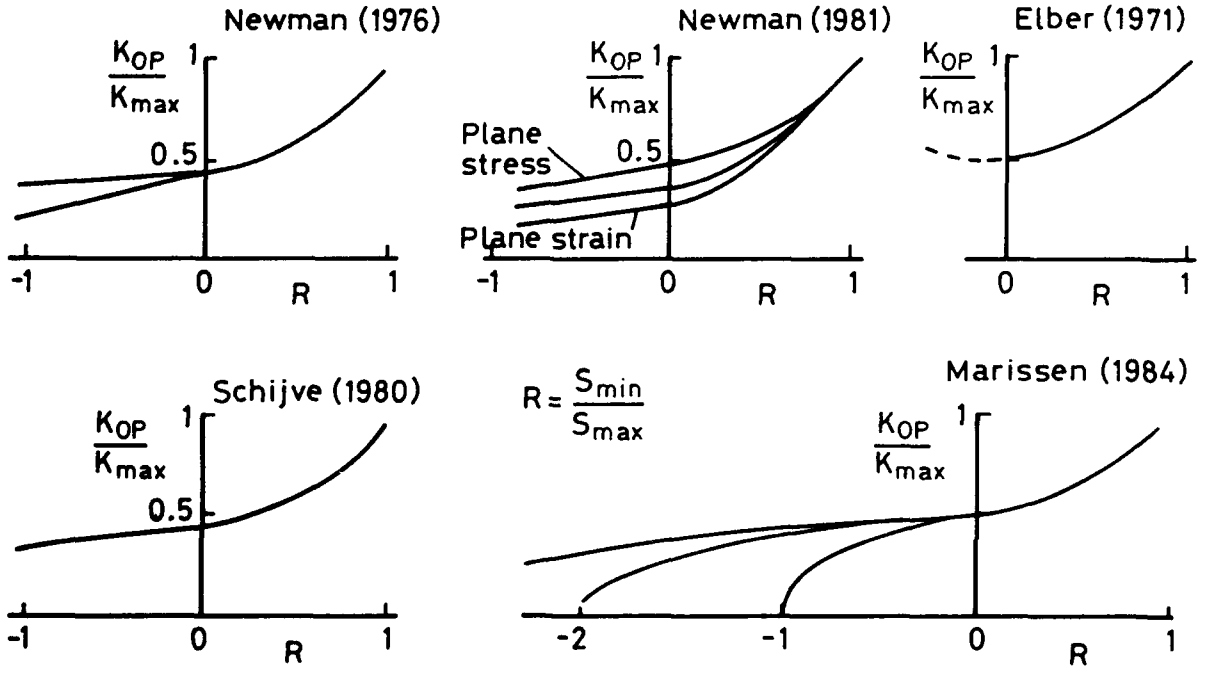

Fig 8b Schematic summary of attempts to relate crack opening to R-ratio (after Marissen *et al*[103])

TR 90046

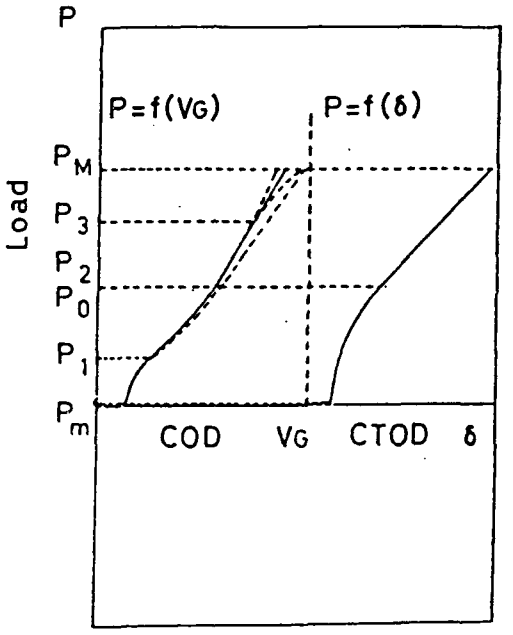

TR 90046

Fig 9 Comparison of load-COD and load-CTOD diagrams, after Clerivet[109]